

Supporting Information

Friedlaender et al. 10.1073/pnas.0905222106

SI Text

SI Methods. Sample preparation. Planarians from the clonal, asexual CIW4 strain of *Schmidtea mediterranea* were starved for 1 week before all experiments. Planarian total RNA was isolated by using the standard TRIzol protocol (Invitrogen). Planarians for the irradiated samples were exposed to 60 Gy in an Irradiator OB29 (STS) and RNA was extracted 8 days after irradiation.

For FACS sorting, *S. mediterranea* were cut twice to release digestive components, rinsed, chopped finely, and dissociated for ≈ 1.5 h at room temperature in a calcium- and magnesium-free salt solution (CMF). The resulting cell suspension was enriched for neoblasts by filtration through nylon fabric of uniform pore size (Nytex) to a maximum of 20 microns, then stained for 30 min at room temperature with Hoechst 33342 and Calcein (Molecular Probes). Stained cells were washed in CMF and propidium iodide was added (1). Single reagent controls were prepared for all reagents. Stained samples were then analyzed on a Becton Dickinson FACSaria fluorescence-activated cell sorter and putative neoblasts were sorted to microcentrifuge tubes containing CMF, after the method of Agata (2). Immediately after sorting cells were pelleted by centrifugation, supernatant was removed, and flash-frozen in liquid nitrogen and stored at -80°C . Eighteen dedicated runs were performed to harvest the neoblasts for generating the small RNA library, with each run of 20 to 30 planaria. A total of 5.6 million cells were accumulated.

Solexa sequencing. Small RNAs from planarian total RNA samples were prepared for Solexa sequencing as follows: ≈ 5 μg total RNA were size-fractionated on 15% TBE-Urea polyacrylamide gel (Sequagel, National Diagnostics) and RNA fragments of lengths between 18 and 40 bases were isolated. Small RNA libraries were prepared by using a modified protocol that prevents small RNA circularization during adapter ligation as described in ref. 3. The purified small RNAs were ligated to preadenylated 3'-adapters by using the mutant RNA ligase Rnl2(1-249)K227Q (3, 4). To remove unligated adapters, the ligation products (40-60 bases in length) were gel purified on 15% TBE-Urea polyacrylamide gel. Subsequently, the RNA fragments with the adapter at the 3' end were ligated with 5'-adapters (Illumina). After gel purification on 15% TBE-Urea polyacrylamide gel, RNA fragments with the adapters at both ends (70-90 bases in length), were reverse transcribed and the resulting cDNA was subjected to 15 PCR cycles. The ≈ 100 base-pair amplification products were gel purified on 15% TBE polyacrylamide gel. The libraries thus obtained were used directly for cluster generation and 36 cycles of sequencing analysis by using the Illumina cluster station and 1G Genome Analyzer following manufacturer protocols. Sequencing reads were extracted from the image files generated by Illumina 1G Genome Analyzer by using the open source Firecrest and Bustard applications (Illumina). The Solexa sequencing of the sample of neoblasts yielded 5,943,990 reads, whereas the sequencing of the untreated and irradiated whole-body neoblast samples yielded 3,772,113 and 4,245,548 reads, respectively.

Preprocessing and mapping of the 454 and Solexa deep-sequencing data. The 454 deep sequencing reads were cleaned of 5' and 3' adapters (CGTAGGCACCTGAAA and CTGTAGGCAC-CATCAA, respectively) by using a custom Perl script searching for near-perfect string matches. Both the sequencing reads and their reverse complements were searched. The Solexa deep-sequencing reads were cleaned of 3'-adapters by using another custom Perl script that searches for the longest instance of the adapter sequence TCGTATGCCGTCTTCTGCTTGT, allow-

ing for 2 edits (mismatches and/or insertions/deletions). The longest instance of adapter sequence searched is 18 nt, meaning that the shortest biological transcripts cleaned of adapters are 16 nt (Solexa read length 36 nt, longest adapter instance searched 18 nt, edit distance 2). Subsequently, 454 and Solexa reads containing >1 uncalled nucleotide or any homo-nucleotides stretches of 7 nt or longer were discarded. The remaining deep sequencing reads were aligned to the planarian genome (*Schmidtea mediterranea*-3.1, from GSC at <http://genome.wustl.edu/>) by using the oligomap application run with the option -m 100 (5). Reads that mapped 100 or more times by using these criteria were discarded, as were suboptimal mappings (edit distance 1 mappings of reads that map perfectly elsewhere on the genome). The following numbers of 454 reads were successfully mapped: 63,278 from neoblasts; 93,412 from untreated; and 61,391 from irradiated. The following numbers of Solexa reads were successfully mapped: 91,371 from neoblasts; 1,784,859 from untreated; and 2,050,669 from irradiated.

Annotating miRNA star strands, rRNA, tRNA, and mRNA. We obtained the available 12 planarian miRNA star strands at miRBase. We used a custom Perl script to annotate the star strands of the remaining miRNAs, integrating precursor secondary structures predicted by RNAfold (6), mature strand coordinates and knowledge of 2 nt 3' overhangs. To annotate *S. mediterranea* rRNA genes, we first obtained the 28S rRNA of this organism at GenBank (7). We blasted this against the nonredundant nucleotide collection at the National Center for Biotechnology Information (NCBI), and noted the Linnaeus names of the 10 flatworms whose 28S rRNA produced the best matches (*Dugesia gonocephala*, *Dugesia sicula*, *Dugesia tigrina*, *Dugesia japonica*, *Neppia sp.*, *Spathula alba*, *Dugesia ryukyensis*, *Dolichoplana sp.*, *Geoplana ladislavii* and *Novibipalium venosum*). We then obtained all available rRNA sequences from these flatworms at GenBank, and blasted these against the *S. mediterranea* genome, by using the NCBI blast application with an e-value cut-off of $1e^{-10}$. The matched genomic regions were annotated as rRNA genes. We annotated tRNA genes by running the tRNAscan-SE-1.23 on the *S. mediterranea* genome with the default eukaryotic parameters. For the mRNA annotation, we used the SmedGD annotation (<http://smedgd.neuro.utah.edu>). Sometimes reads mapped to more than one type of annotation. In these cases, we resolved annotation by a confidence-based hierarchy: miRNA $>$ mRNA $>$ tRNA $>$ rRNA $>$ piRNA. This strategy is comparable to the one used in ref. 5.

Comparing sets of piRNAs. We obtained the set of piRNAs previously discovered by Palakodeti et al. (8). We then mapped these piRNAs against our pooled deep-sequencing datasets by using a custom mapping tool, allowing for 2 edits (mismatches and/or insertions/deletions). Of 4,485 piRNAs previously reported, we found matches for 1,684 (38%).

Calculating read mapping and overlap intensities. For the purposes of piRNA analysis, all read mappings were assigned intensities that were inverse to the number of times the given read mapped to the genome. For instance, a read mapping 100 times would have each mapping assigned an intensity of 0.01. This is equivalent to weighing the mappings. When 2 reads overlapped, the overlap was assigned an intensity that is the mean of the intensities of the 2 reads in log-space. For instance, the overlap between 2 read mappings with intensity 0.1 would be weighted 0.1, as would the overlap between one read mapping with intensity 1 and one with intensity 0.01.

piRNA repeat association. We downloaded the latest version of RepBase (9) and scanned the planarian genome for repeats by using RepeatMasker with the following options: -s -species "schmidtea mediterranea" -gccalc -xsmall. To quantify piRNA enrichment, we compared the fraction of piRNAs that overlaps with repeat annotations with the fraction of the planarian genome that is covered by the same repeat annotations. If the fraction of piRNAs covered by the repeats was larger than expected from the genome coverage of the repeats, we noted the repeats as enriched in piRNAs. This analysis was done for each class of repeats and for the total set of repeats. The set of piRNAs from the untreated planarian sample was used for this analysis. To test whether the piRNA enrichment or depletion of a given transposon type is significant, we used binomial statistics. We set the number of trials n as the number of piRNA reads and the probability of success p as the probability that a piRNA overlaps with the transposon type. The probability p was set equal to the genome coverage of the transposon type (taking into account edge effects of the overlaps). We also made controls by randomly shuffling the annotated repeats to new positions on the same contig strand and comparing with piRNA mappings, with similar results.

Control for false positives in the piRNA cluster analysis. It was important to check that genomic clusters of mapped reads would not be flagged as piRNA clusters if reads would distribute randomly to the genome. We thus moved each individual read to a random position in the genome and repeated the cluster identification procedure. This control did not yield any clusters.

Prediction of novel planarian miRNAs by using miRDeep. Because it is known that miRNA mature and star strands map few times to metazoan genomes, deep-sequencing reads that mapped >5 times were disregarded for purposes of miRNA prediction. The remaining reads were used as guidelines for excising potential precursor sequences from the genome, and these were filtered and scored by the miRDeep core algorithm as previously described (10). We further improved the prediction by taking 2 extra measures: (i) potential precursors were only excised if the putative mature miRNA was represented by 2 or more perfectly mapping reads, and (ii) a limited set of known mature miRNAs from miRBase was used for purposes of seed conservation. Only mature sequences belonging to families present in invertebrates or that are present in both mammalian and nonmammalian vertebrates were used for conservation scoring. A cut-off of 1 was used for both the 454 and the Solexa data. Redundancy in the predictions caused by errors in the genome assembly was removed by manual curation. No reads were initially discarded based on annotation, but comparison between the predictions and genome annotations revealed that 1 prediction overlapped with a rRNA gene. This prediction was removed. Permutation controls were performed as previously described (10). Table S6 gives an overview of the novel planarian miRNAs. Fig. S3 gives an overview of the family relations and phylogeny of all planarian miRNAs.

Northern blot analysis. Validation of miRNA or piRNA candidates was performed by Northern blot analysis as described earlier (11). In brief, 30 to 50 μ g total RNA and an RNA ladder (Decade Markers, Ambion) were resolved side by side on a 15% TBE-Urea polyacrylamide gel (Sequagel, National Diagnostics). Hybridization and wash steps were performed at 43–45 °C. The ³²P-radiolabeled oligodeoxynucleotide probes are described in Table S8.

Real time RT-PCR (qPCR). Thirty-eight planarian custom TaqMan miRNA assays designed for mature miRNA quantification (Applied Biosystems) were used in this study.

cDNA was synthesized from 50 ng total RNA from either irradiated or untreated worms in a 15- μ L reaction volume according to TaqMan MicroRNA Assay protocol, by using hairpin primers targeting specifically mature miRNAs. Reverse

transcription was performed by using the following program: 30 min at 16 °C, 30 min at 42 °C, 5 min at 85 °C and then held at 4 °C. Samples without reverse transcriptase served as the negative control template. For relative quantification by real time, 1.5 μ L cDNA were used in a total reaction volume of 20 μ L with 1 μ L custom TaqMan assay by using an Applied Biosystems StepOne Real-Time PCR System. Thermal cycling program used for quantification was as follows: 50 °C for 2 min and 95 °C for 10 min, followed by 40 cycles of 95 °C for 15 s and 60 °C for 1 min.

For miRNA quantification, it is utterly important to select the right endogenous control to circumvent normalization on total RNA. Noncoding RNAs are the controls of choice in real time PCR assays, i.e., ribosomal RNAs, snoRNAs, or snRNAs. We first used U6, but its level of expression was too low to get an adequate amplification with our methodology. U6 assays also showed that U6 levels were not constant across samples. Other groups have often used another miRNA as an internal control, one observed to have steady level of expression across samples based on total RNA input in preliminary studies. We decided however that such control could bring strong biases. Thus, the constitutively expressed gene *ura4* (accession number: AY068123) was selected in this study as an endogenous control (1). Sets of specific *ura4* primers and a TaqMan probe (Applied Biosystems) were designed to target an exon–exon junction. cDNA was synthesized from 50 ng total RNA from untreated or from irradiated worms with 0.5 μ M final oligo(dT)₂₀ in a 20 μ L reaction by using the following program: 5 min at 25 °C, 30 min at 42 °C, 5 min at 85 °C and then held at 4 °C. Real time was conducted on the endogenous control with the exact same conditions used in the miRNA assays described above and run in parallel.

Each measurement was performed in triplicate and no-template controls were included for each assay. At least 2 biological replicates were used in the study. Data were analyzed by using StepOne v2.0 software (Applied Biosystems). *Ct* (threshold cycle) values of real-time PCR were normalized to the endogenous control which was measured in parallel. The relative expression of each miRNA between irradiated and untreated samples is given as \log_2 of $2^{-\Delta\Delta Ct}$ values.

As an additional control and to check that miRNA down regulation was due to neoblast depletion and not to the γ -radiation treatment, we performed in parallel the exact same experiments on a neoblast-enriched cell fraction. Planarians were chopped into small pieces in 500 μ L Accutase (Millipore), placed into 5.5 mL Accutase solution, and left to rock for 2 h at room temperature until complete dissociation. The dissociated cells were placed on ice, collected by centrifugation at 4 °C, and resuspended in 10 mL cold CMF (15 mM Hepes, 400 mg/L NaH₂PO₄, 800 mg/L NaCl, 1200 mg/L KCl, 800 mg/L, NaHCO₃, 240 mg/L glucose, pH 7.3). To obtain the neoblast-enriched cell fraction, cells were filtrated serially through a 70- μ m nylon filter (BD Falcon), a 40- μ m nylon filter (BD Falcon) and a 20- μ m nylon filter (Millipore). Filtrated cells were collected by centrifugation and RNA was extracted using TriZol (Invitrogen) following the manufacturer protocol.

Smedwi-1 mRNA relative expression was assayed by real time PCR on total RNA extracted from filtrated cells, untreated planarians, and irradiated planarians by using *ura4* as an endogenous control and following the protocol described above for the *ura4* gene. Smedwi-1 expression was greatly reduced in the irradiated sample (400-fold down) and increased in the filtrated cells (1.8-fold up).

A 1-to-1 correlation was found between all miRNAs that went significantly down in the neoblast-depleted sample (irradiated planarians) and significantly up in the neoblast-enriched sample (filtrated cells). These results demonstrate that miRNA down regulation in irradiated planarians is not due to γ -radiation effects but to the depletion of neoblasts.

Quantifying total miRNA and piRNA expression. The total expression of miRNAs and piRNAs in the 3 samples was performed by normalizing to 3 miRNAs that were constant in the 3 samples according to qPCR (miR-71c, miR-36, and miR-36c). The 454 data, produced by specifically sequencing small RNAs of 18–25 nt in length, was used to estimate miRNA expression, whereas the Solexa data were used to estimate piRNA expression. Total miRNA and piRNA read counts were normalized by dividing by the read count of the constantly expressed miRNA. The miRNA and piRNA expression of the untreated sample was set to 1, and the other expression levels were scaled accordingly (Table S3).

Quantifying expression of individual miRNAs from deep-sequencing data. We intersected the genome coordinates of all mapped reads with the genome coordinates of all planarian miRNA mature and star strands. If a mapped read was fully contained within the genome coordinates of a miRNA strand, including 5 nucleotide flanks upstream and downstream, then it was assumed to be the sequencing product of the strand, and was counted toward the read count of the miRNA. Because suboptimal mappings were discarded (see above), a given read was only mapped to >1 miRNA gene if the genes had identical mature sequences. Table S1 gives an overview of miRNA counts in the 6 datasets. When fold-changes between samples were calculated, the read counts of individual miRNAs in a sample were normalized by dividing by the total miRNA read count in the sample.

SI Results. miRNA analysis and phylogeny. We searched the 454 and the Solexa data separately with miRDeep (SI Methods). The default cut-off was found to recover miRNA hairpins with high sensitivity (83% for the 454 data and 84% for the Solexa data). The numbers of false positives were estimated computationally as previously described (10) and were found to be low (6 ± 2 s.d. and 7 ± 3 s.d. false positives for the 454 and Solexa data, respectively). In total, 90 and 118 unique hairpins exceeded the score cut-off. Of these, 52 and 53 represented known miRNA hairpins, whereas 38 and 65 represented novel planarian miRNA hairpins. Because there was significant overlap between the miRNAs detected in the 2 types of deep-sequencing data, we report a total number of 70 novel miRNAs. Curation showed that 1 reported miRNA had short loop untypical of Dicer processing. It was therefore omitted from further analysis. The planarian miR-753 and miR-754 families both had several family members with high sequence similarity. Although these miRNAs were individually plausible, only a subset were supported by uniquely mapping reads. To err on the side of caution, we therefore omitted the remaining 8 miRNAs from the main body of the manuscript, although they are retained in Table S6.

We find that planarians share miRNA families with flies, nematodes, and mammals (Fig. S3). For example, our data show that there are 3 *lin-4*/miR-125 and 4 *let-7* homologs in *S. mediterranea*. The *lin-4* and *let-7* families of miRNAs are often present in multiple copies in a genome and are highly conserved across species in sequence and function, i.e., cell differentiation and proliferation (for review see ref. 12). Moreover, *let-7* is posttranscriptionally regulated by *lin-28* (13), an RNA-binding protein that can be used to help reprogram mammalian somatic-differentiated cells into embryonic stem cells (14). Among other miRNA genes deeply conserved in the animal taxa, we report also 4 miRNAs belonging to the miR-1 family and 5 belonging to the miR-124 family. The miR-124 miRNAs are highly conserved and expressed specifically in the developing and adult nervous systems (15) where they promote neuronal differentiation (16, 17). The function of miR-1 in the differentiation of skeletal muscle is conserved from human to fly (18). Because planarians are among those metazoans in which muscle is neither smooth nor striated (19), it will be interesting to investigate the function of these 4 family members.

Interestingly, we find that the majority of planarian miRNA

families do not show sequence similarity to any known miRNAs (Fig. S3). These families might be common to lophotrochozoans or might be specific to planarians. In either case, they underline the need for further molecular and genetic exploration of the Lophotrochozoa, a superphylum representing the largest collection of metazoan body plans.

Genomic organization of planarian miRNA genes. In mammals, flies, and nematodes, the transcriptional regulation of miRNAs is complicated, with many miRNA genes being part of larger transcription units. In contrast, the genomic positions of planarian miRNAs suggest that most are independently transcribed. For instance, only 3 of 124 (2%) planarian miRNA genes are intronic, whereas this percentage is much higher for humans (45%), *D. melanogaster* (43%), and *C. elegans* (36%). Planarians have 28 (23%) miRNAs that locate to miRNA gene clusters, whereas relatively more miRNAs are clustered in human (38%), fly (46%), and nematode (31%). However, given the fragmented nature of the planarian genome draft assembly, we cannot rule out an underestimation of clustered or intronic miRNAs.

Planarian piRNAs and their associated Piwi proteins. The predominant length of planarian piRNAs is 32 nt, longer than observed in other species, and this may be the result of the “footprint” of planarian PIWI proteins. The *S. mediterranea* genome contains 3 piwi-like genes, *smedwi-1* to *-3*. SMEDWI-1 and *-2* have been shown previously to be specifically expressed in neoblasts (1) and SMEDWI-2 and *-3* are required for regeneration and stem cell differentiation (1, 8). SMEDWI-1 and SMEDWI-2 proteins have high sequence similarity to each other and to the *D. japonica* PIWI-like protein DjPIWI-1 (20), whereas SMEDWI-3 is more closely related to *D. melanogaster* AGO-3 than SMEDWI-1 and *-2*. In mammals and flies, the sequence biases of piRNA subpopulations reflect association with distinct PIWI proteins, and the same may hold true in planarians. Therefore, we recognize that PIWI protein pull-downs and possibly more cell sorting will be necessary to deconvolute all subpopulations.

Long and short piRNAs. The set of reads annotated as long (>25 nt) piRNAs seem to constitute a homogenous population of small RNAs because the peaked length profile in Fig. 2C is smooth, indicating small RNAs generated by the same mechanism. The short piRNAs have similar features as the long piRNAs, but less pronounced (10 nt overlap, transposon association biases). We attempted to estimate the dilution of genuine piRNAs in the set of short piRNA set by simulation. First we randomly sampled the long piRNA mappings to make them comparable in number to the short piRNA mappings. Then we substituted, at random, individual long piRNA mappings with mappings to random positions in the genome, simulating dilution with transcripts not associated with piRNA biology. We found that the long piRNA mappings, when 20–30% of dilution was simulated, had a 10-nt overlap peak of the same height as that of the (untouched) short piRNA mappings. Similarly, we found that the long piRNA mappings with simulated 20–30% dilution had similar biases in transposon association as do the short piRNA mappings. Therefore, we estimate that the sets of reads annotated as short piRNAs contain 20–30% nonpiRNA sequences. This holds for both untreated and irradiated planarians.

Analysis of genic piRNAs. We discovered that substantial numbers of deep-sequencing reads map to annotated exons of protein-coding genes. For instance, in Solexa sequencing data of untreated planarians, we found $\approx 80,000$ reads that map to exons, about one-third of which map antisense. These reads display features of planarian piRNAs, such as a length profile peaking at 32 nt, a tendency to overlap by 10 nt, and sequence biases resembling those of primary piRNAs (antisense) or secondary piRNAs (sense). Similar observations have previously been made in planarians (8) and in vertebrates such as zebrafish (21), and are consistent with a model in which gene transcripts being regulated by antisense piRNAs. To rule out that these genic

piRNAs are artifacts due to genome misannotations or ambiguous read mappings, we performed a rigorous analysis of deep sequencing reads mapping to exons and introns. We counted up the numbers of long (>25 nt) reads that could be traced unambiguously to the following types of annotation: intergenic (the entire genome excluding genes and piRNA clusters), exons of protein coding genes, exons of conserved protein coding genes (true homologs of human genes, analysis as in ref. 22), introns of protein coding genes, introns of conserved protein coding genes, and our annotated piRNA clusters (Table S2).

This more rigorous analysis yielded unforeseen results. First, we found that both exons and introns have fewer reads mapping

antisense per kb than do genome strands of the intergenic background. Exons are depleted in antisense reads by a factor of 7, whereas introns are depleted by a factor of 3, suggesting that there is in fact a general selection pressure to avoid short RNAs with perfect complementarity to gene transcripts. Second, when we manually investigated exons that have multiple reads mapping antisense, we found that the exons in the gene models were possible misannotations, i.e., nonconserved exons in otherwise conserved genes. Third, the genes that have reads mapping antisense were not enriched in any gene ontology. In sum, we find little evidence that planarian gene transcripts are targeted by antisense piRNAs.

1. Reddien PW, Oviedo NJ, Jennings JR, Jenkin JC, Sanchez Alvarado A (2005) SMEDWI-2 is a PIWI-like protein that regulates planarian stem cells. *Science* 310:1327–1330.
2. Hayashi T, Asami M, Higuchi S, Shibata N, Agata K (2006) Isolation of planarian X-ray-sensitive stem cells by fluorescence-activated cell sorting. *Dev Growth Differ* 48:371–380.
3. Hafner M, et al. (2008) Identification of microRNAs and other small regulatory RNAs using cDNA library sequencing. *Methods* 44:3–12.
4. Ho CK, Wang LK, Lima CD, Shuman S (2004) Structure and mechanism of RNA ligase. *Structure* 12:327–339.
5. Berninger P, Gaidatzis D, van Nimwegen E, Zavolan M (2008) Computational analysis of small RNA cloning data. *Methods* 44:13–21.
6. Hofacker IL (2003) Vienna RNA secondary structure server. *Nucleic Acids Res* 31:3429–3431.
7. Benson DA, Karsch-Mizrachi I, Lipman DJ, Ostell J, Wheeler DL (2004) GenBank: Update. *Nucleic Acids Res* 32:D23–D26.
8. Palakodeti D, Smielewska M, Lu YC, Yeo GW, Graveley BR (2008) The PIWI proteins SMEDWI-2 and SMEDWI-3 are required for stem cell function and piRNA expression in planarians. *RNA* 14:1174–1186.
9. Jurka J (2000) Repbase update: A database and an electronic journal of repetitive elements. *Trends Genet* 16:418–420.
10. Friedlander MR, et al. (2008) Discovering microRNAs from deep sequencing data using miRDeep. *Nat Biotechnol* 26:407–415.
11. Lagos-Quintana M, Rauhut R, Lendeckel W, Tuschl T (2001) Identification of novel genes coding for small expressed RNAs. *Science* 294:853–858.
12. Roush S, Slack FJ (2008) The let-7 family of microRNAs. *Trends Cell Biol* 18:505–516.
13. Viswanathan SR, Daley GQ, Gregory RI (2008) Selective blockade of microRNA processing by Lin28. *Science* 320:97–100.
14. Yu J, et al. (2007) Induced pluripotent stem cell lines derived from human somatic cells. *Science* 318:1917–1920.
15. Lagos-Quintana M, et al. (2002) Identification of tissue-specific microRNAs from mouse. *Curr Biol* 12:735–739.
16. Visvanathan J, Lee S, Lee B, Lee JW, Lee SK (2007) The microRNA miR-124 antagonizes the anti-neural REST/SCP1 pathway during embryonic CNS development. *Genes Dev* 21:744–749.
17. Makeyev EV, Zhang J, Carrasco MA, Maniatis T (2007) The MicroRNA miR-124 promotes neuronal differentiation by triggering brain-specific alternative pre-mRNA splicing. *Mol Cell* 27:435–448.
18. Nguyen HT, Frasch M (2006) MicroRNAs in muscle differentiation: Lessons from *Drosophila* and beyond. *Curr Opin Genet Dev* 16:533–539.
19. Sarnat HB (1984) Muscle histochemistry of the planarian *Dugesia tigrina* (Turbellaria: Tricladia): Implications in the evolution of muscle. *Trans Am Microsc Soc* 103:284–294.
20. Rossi L, et al. (2006) DjPiwi-1, a member of the PAZ-Piwi gene family, defines a subpopulation of planarian stem cells. *Dev Genes Evol* 216:335–346.
21. Houwing S, Berezikov E, Ketting RF (2008) Zili is required for germ cell differentiation and meiosis in zebrafish. *EMBO J* 27:2702–2711.
22. Moreno-Hagelsieb G, Latimer K (2008) Choosing BLAST options for better detection of orthologs as reciprocal best hits. *Bioinformatics* 24:319–324.
23. Palakodeti D, Smielewska M, Graveley BR (2006) MicroRNAs from the Planarian *Schmidtea mediterranea*: A model system for stem cell biology. *RNA* 12:1640–1649.
24. Wheeler BM, et al. (2009) The deep evolution of metazoan microRNAs. *Evol Dev* 11:50–68.
25. Peterson KJ, Dietrich MR, McPeck MA (2009) MicroRNAs and metazoan macroevolution: Insights into canalization, complexity, and the Cambrian explosion. *Bioessays* 31:736–747.

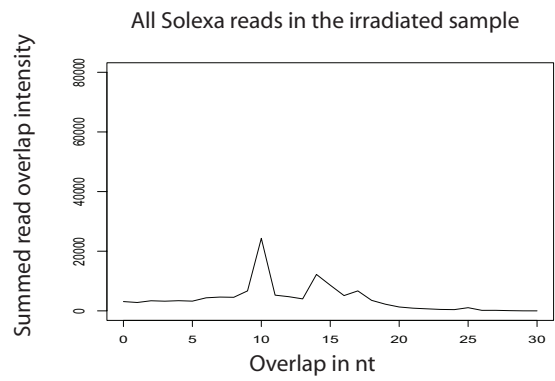


Fig. S1. Summed overlap intensities for all Solexa reads in the irradiated sample. The horizontal axis is the length of overlap in nucleotides between the 5' ends of reads mapping to the same genomic locus on opposite strands. The vertical axis shows the intensity of the overlap, summed over the entire dataset.

Metazoan miRNA families:					
miR-10/100:	Mature sequence	Reads:	Star	Validation:	
sme-miR-10	ACCCUGGAGAUCCGAGUUUGA	51155	1412	B, P	
sme-miR-10a	ACCCUGGAGAUCCGAGUUUGA	34713	4455		
Bilateria miRNA families:					
let-7:					
sme-let-7a	UGAGGUAGAAUUGUGAUGACU	33509	173	B, P	
sme-let-7b	UGAGGUAGAAUUGUGAUGACU	27639	612	B, P	
sme-let-7c	UGAGGUAGAAUUGUGAUGACU	17967	20	P	
sme-let-7d	AGAGGUAGAAUUGUGAUGACU	1887	51	B, P	
lin-4/miR-125:					
sme-lin-4	UCCUGGAGACUUGGACUGUGU	16607	4643	B, P	
sme-miR-125a	UCCUGGAGACUUGGACUGUGU	3733	83		
sme-miR-125b	UCCUGGAGACUUGGACUGUGU	8158	4898		
miR-1:					
sme-miR-1a	UGGAUUGUCGAAUUGGACU	28990	296	B, P	
sme-miR-1b	UGGAUUGUCGAAUUGGACU	19237	3791	B, P	
sme-miR-1c	UGGAUUGUCGAAUUGGACU	90159	491	B, P	
miR-7:					
sme-miR-7a	UGGAAGACUUAUUGUUAUGA	360	10		
sme-miR-7b	UGGAAGACUUAUUGUUAUGA	2967	17		
sme-miR-7c	UGGAAGACUUAUUGUUAUGA	6300	107		
sme-miR-7d	UGGAAGACUUAUUGUUAUGA	396	6		
miR-8:					
sme-miR-8	UAUAUCUGGACGUAACGAGCC	3526	990	B	
sme-miR-8b	UAUAUCUGGACGUAACGAGCC	5034	13	B	
miR-9:					
sme-miR-9a	UCUUUGUUAUUGGACUGUUAUGA	7036	80	P	
sme-miR-9b	UCUUUGUUAUUGGACUGUUAUGA	1774	149		
miR-22/745/980:					
sme-miR-745	UGCUGGACUUAUUGGACUGUUAUGA	14957	162	B	
miR-31:					
sme-miR-31a	AGGCCAAGUUGGACUAACUGA	2240	434	B	
sme-miR-31b	AGGCCAAGUUGGACUAACUGA	1758	33	B	
miR-71:					
sme-miR-71a	UGAAAGACACAGGUAUGGAC	17436	192	B, P	
sme-miR-71b	UGAAAGACACAGGUAUGGAC	28572	311	B, P	
sme-miR-71c	UGAAAGACACAGGUAUGGAC	10828	63	B, P	
miR-96:					
sme-miR-96a	UUUGGCAUUUAGGAAUUGGACU	9400	71		
sme-miR-96b	UUUGGCAUUUAGGAAUUGGACU	9141	3		
miR-124:					
sme-miR-124a	UAAGGCACCGGUAAGGACU	2480	22	B	
sme-miR-124b	UAAGGCACCGGUAAGGACU	2622	29	B	
sme-miR-124c	UAAGGCACCGGUAAGGACU	3976	64	B	
sme-miR-124d	UAAGGCACCGGUAAGGACU	81	8	B	
sme-miR-124e	UAAGGCACCGGUAAGGACU	216	17	B	
miR-133:					
sme-miR-133	UUGGUCACCAUAGGACUGU	468	19	P	
sme-miR-133a	UUGGUCACCAUAGGACUGU	160	11	P	
miR-190:					
sme-miR-190a	AGAAUUGUUUGUUAUUGGUGA	57531	8531		
sme-miR-190b	AGAAUUGUUUGUUAUUGGUGA	4437	5990		
other families:					
sme-miR-79	CUAAAGCUAAUUAACCAAGUC	10276	1279		
sme-miR-92	CUAUGGACUUAUUGGACU	1062	546	B, P	
sme-miR-184	GACGGAGUUUGUAAGGAA	1991	174		
sme-miR-216	CAUUCUGGACUUAUUGGACU	2169	2954	P	
sme-miR-219	UGAUCUUGGACUUAUUGGACU	5829	317		
sme-miR-278	UGGUCUUGGACUUAUUGGACU	14536	606	B	
sme-miR-281	UGGUCUUGGACUUAUUGGACU	20697	216	B	
sme-miR-315	UUUUGAUUUUGGACUUAUUGGACU	2719	14		
Protostome miRNA families:					
bantam:					
sme-bantam-a	UGAGAUACUUAUUGGACU	103756	1197	B, P	
sme-bantam-b	UGAGAUACUUAUUGGACU	21017	134	B, P	
sme-bantam-c	UGAGAUACUUAUUGGACU	1477	35	B, P	
miR-213:					
sme-miR-2a	UAUCAGAGCCCGUUGGACUGU	20830	707	B, P	
sme-miR-2b	UAUCAGAGCCCGUUGGACUGU	5937	5040	B, P	
sme-miR-2c	UAUCAGAGCCCGUUGGACUGU	10336	2776	B, P	
sme-miR-2d	UAUCAGAGCCCGUUGGACUGU	16920	2798	B, P	
sme-miR-13	UAUCAGAGCCCGUUGGACUGU	9933	171	B, P	
Protostome miRNA families (continued):					
miR-36:					
sme-miR-36	UCACCGGUGAGCAUUAUUGA	18240	4421	P	
sme-miR-36b	UCACCGGUGAGCAUUAUUGA	2422	118	B, P	
sme-miR-36c	UCACCGGUGAGCAUUAUUGA	7017	286	P	
miR-87:					
sme-miR-87a	UGAGCAAGUUUUAUUGGACU	1879	141		
sme-miR-87b	UGAGCAAGUUUUAUUGGACU	1647	558		
sme-miR-87c	UGAGCAAGUUUUAUUGGACU	1532	114	B	
sme-miR-87d	UGAGCAAGUUUUAUUGGACU	440	242	B	
miR-277:					
sme-miR-277a	UAAUUGGACUUAUUGGACU	19321	392	B	
sme-miR-277b	UAAUUGGACUUAUUGGACU	3521	811	B	
sme-miR-277c	UAAUUGGACUUAUUGGACU	8296	82	B	
sme-miR-277d	UAAUUGGACUUAUUGGACU	9790	1358	B	
miR-279/61:					
sme-miR-61	UGACUAGAAUUGGACUUAUUGGACU	22896	109		
sme-miR-61b	UGACUAGAAUUGGACUUAUUGGACU	943	4527		
other families:					
sme-miR-12	UAGAUUCUUAUUGGACUUAUUGGACU	1948	37		
sme-miR-67	UACACAGUUAUUGGACUUAUUGGACU	5751	467		
sme-miR-750	UAGAUUCUUAUUGGACUUAUUGGACU	21924	347	B	
sme-miR-1175	UGAGAUUCUUAUUGGACUUAUUGGACU	1560	2659		
sme-miR-1993	UAUUAUGGACUUAUUGGACUUAUUGGACU	9196	1098	B, P	
Lophotrochozoan miRNA families:					
miR-1992:					
sme-miR-1992	UCAGCAGUUAUUGGACUUAUUGGACU	316	142	B	
S. mediterranea miRNA families with no known conservation:					
miR-753:					
sme-miR-753	GAGCUUGGACUUAUUGGACUUAUUGGACU	902	505		
sme-miR-753b	AGCCUUGGACUUAUUGGACUUAUUGGACU	451	730		
miR-754:					
sme-miR-754	GUUUCUUUGGACUUAUUGGACUUAUUGGACU	108	29		
sme-miR-754b	GUUUCUUUGGACUUAUUGGACUUAUUGGACU	860	7	B	
sme-miR-754c	GUUUCUUUGGACUUAUUGGACUUAUUGGACU	761	30		
miR-2147:					
sme-miR-2147a	CGGAAAGCUCGACGACGAC	34	97		
sme-miR-2147b	CGGAAAGCUCGACGACGAC	160	6		
sme-miR-2147c	CGGAAAGCUCGACGACGAC	630	11		
other families:					
sme-miR-746	UAGCACCAGGUAUUAUUGGACUUAUUGGACU	3220	1303		
sme-miR-747	UAUUCUUAUUGGACUUAUUGGACUUAUUGGACU	9557	3059		
sme-miR-748	UGGACCGAAUUGGACUUAUUGGACUUAUUGGACU	13340	24	B	
sme-miR-749	CGUCGAAUUGGACUUAUUGGACUUAUUGGACU	176	10		
sme-miR-751	CAUUAUUGGACUUAUUGGACUUAUUGGACU	6058	0		
sme-miR-752	AGUCAGUUAUUGGACUUAUUGGACUUAUUGGACU	738	2374	P	
sme-miR-755	UGGACUUAUUGGACUUAUUGGACUUAUUGGACU	2780	8287	B	
sme-miR-756	CGAAUUGGACUUAUUGGACUUAUUGGACU	3658	223	B, P	
sme-miR-2148	AGAAUUCUUAUUGGACUUAUUGGACU	271	11		
sme-miR-2149	CGCAGAAUUGGACUUAUUGGACUUAUUGGACU	405	208		
sme-miR-2150	CGGUUACGUAUUAUUGGACUUAUUGGACU	57	41		
sme-miR-2151	GAUUCAGUUAUUGGACUUAUUGGACUUAUUGGACU	14130	265	B, P	
sme-miR-2152	GGGUUCGAAUUGGACUUAUUGGACUUAUUGGACU	497	16	B	
sme-miR-2153	UAGCAGUUAUUGGACUUAUUGGACUUAUUGGACU	935	389		
sme-miR-2154	UCAGCAGUUAUUGGACUUAUUGGACUUAUUGGACU	10012	48	B	
sme-miR-2155	GACACUUAUUGGACUUAUUGGACUUAUUGGACU	3	0		
sme-miR-2156	UCUUCAGCAGUUAUUGGACUUAUUGGACUUAUUGGACU	539	43	B	
sme-miR-2157	UGAAUUGGACUUAUUGGACUUAUUGGACUUAUUGGACU	9113	14		
sme-miR-2158	UGAAUUGGACUUAUUGGACUUAUUGGACUUAUUGGACU	1676	163		
sme-miR-2159	UGGCUUAUUGGACUUAUUGGACUUAUUGGACU	3809	223		
sme-miR-2160	UGGCGUUAUUGGACUUAUUGGACUUAUUGGACU	144	0	P	
sme-miR-2161	UGGCGUUAUUGGACUUAUUGGACUUAUUGGACU	259	4	P	
sme-miR-2162	UGGCGUUAUUGGACUUAUUGGACUUAUUGGACU	4465	441		
sme-miR-2163	UGGCGUUAUUGGACUUAUUGGACUUAUUGGACU	438	127	P	
sme-miR-2164	UGGCGUUAUUGGACUUAUUGGACUUAUUGGACU	1736	324		
sme-miR-2165	UAAUUGGACUUAUUGGACUUAUUGGACUUAUUGGACU	1046	192		
sme-miR-2166	UGGUCUUAUUGGACUUAUUGGACUUAUUGGACU	10	9		
sme-miR-2167	UGGUCUUAUUGGACUUAUUGGACUUAUUGGACU	94	1		
sme-miR-2168	UAUUCUUAUUGGACUUAUUGGACUUAUUGGACU	112	37		
sme-miR-2169	ACUUUGGACUUAUUGGACUUAUUGGACUUAUUGGACU	45	16		
sme-miR-2170	ACAGUUAUUGGACUUAUUGGACUUAUUGGACU	24	5		
sme-miR-2171	UGGUCUUAUUGGACUUAUUGGACUUAUUGGACU	48	3		
sme-miR-2172	UACAGUUAUUGGACUUAUUGGACUUAUUGGACU	8	5		
sme-miR-2173	UACAGUUAUUGGACUUAUUGGACUUAUUGGACU	150	3		
sme-miR-2174	AUUUCGUGGACUUAUUGGACUUAUUGGACU	52	3		
sme-miR-2175	UACUUAUUGGACUUAUUGGACUUAUUGGACU	4	2		
sme-miR-2176	AGAAUUGGACUUAUUGGACUUAUUGGACU	4	9		
sme-miR-2177	AAUUGGACUUAUUGGACUUAUUGGACUUAUUGGACU	43	17		
sme-miR-2178	UAUUGGACUUAUUGGACUUAUUGGACUUAUUGGACU	1294	2		
sme-miR-2179	AGAAUUGGACUUAUUGGACUUAUUGGACUUAUUGGACU	1259	6		
sme-miR-2180	UGGAAUUGGACUUAUUGGACUUAUUGGACUUAUUGGACU	53	0		
sme-miR-2181	UAUUGGACUUAUUGGACUUAUUGGACUUAUUGGACU	75	0		

Fig. S3. Phylogeny and family relations of planarian miRNAs. miRNAs in yellow are novel genes reported in this study, whereas miRNAs in dark green were reported by Palakodeti et al. (23). The relative depth of conservation of the miRNA families is indicated by the color saturation, such that more deeply conserved families have a deeper color. A number of the validations by Northern blot analysis shown in this figure were performed in this previous study. "B" indicates that the mature miRNA was validated by Northern blot analysis either by Palakodeti et al. or in this study, whereas "B2" indicates that validation was performed independently in both studies. "P" indicates that the mature miRNA was validated by Taqman qPCR assay using custom primers (current study). Read numbers refer to the entire sequencing data, pooled from all samples that were obtained in this study. All miRNA names and family relations were assigned by miRBase curators, based on analysis of seed sequences and overall mature miRNA sequence similarity. Consensus family seed sequences are boxed in. Phylogeny of the planarian miRNA families was based on the study by Wheeler et al. (24) and the study by Peterson et al. (25). The one "metazoan" miRNA family (miR-10/100) is inferred in this study to have originated in the eumetazoan ancestor. The 21 "bilateria" families are inferred to have originated in the triboloblastic or in the nephrozoan ancestor. The 11 "protostome" families are inferred to have originated in the protostome ancestor. The "lophotrochozoan" family (miR-1992) is inferred to have originated in the eutrochozoan ancestor. Forty-five miRNA planarian families appeared unrelated to miRNAs in other species.

Table S1. Expression of all annotated planarian miRNA genes in the 6 deep-sequencing datasets as measured by read counts

miRNA genes	454			Solexa		
	Neoblast	Untreated whole-body	Irradiated whole-body	Neoblast	Untreated whole-body	Irradiated whole-body
sme-bantam-a	4	25	11	27	45,940	57,749
sme-bantam-a*	0	60	35	0	449	653
sme-bantam-b	453	1,546	848	7	81,10	10,053
sme-bantam-b*	0	0	0	2	59	73
sme-bantam-c	5	2	6	7	670	787
sme-bantam-c*	1	1	0	1	13	19
sme-let-7a	78	88	20	337	24,510	8,476
sme-let-7a*	1	10	2	2	68	90
sme-let-7b	147	189	61	162	14545	12,535
sme-let-7b*	1	2	0	1	222	386
sme-let-7c	905	1,797	949	2	6,187	8,127
sme-let-7c*	0	0	0	0	11	9
sme-let-7d	35	68	24	333	795	632
sme-let-7d*	0	0	0	0	31	20
sme-lin-4	622	834	453	9	6,073	8,616
sme-lin-4*	12	209	108	10	1,551	2,753
sme-miR-10	5	52	21	218	24,300	56,560
sme-miR-10*	1	57	20	0	420	914
sme-miR-10a	3	48	20	28	9,717	24,897
sme-miR-10a*	0	0	0	4	1,499	2,952
sme-miR-1175	8	143	94	0	259	1,056
sme-miR-1175*	0	13	3	0	721	1,922
sme-miR-12	30	1,136	732	0	162	400
sme-miR-12*	0	3	0	0	10	9
sme-miR-124a	53	300	202	0	789	1,278
sme-miR-124a*	0	1	1	1	8	18
sme-miR-124b	106	424	256	2	1,250	1,938
sme-miR-124b*	0	23	16	0	8	17
sme-miR-124c	263	1,364	793	0	478	835
sme-miR-124c*	0	4	1	0	32	46
sme-miR-124d	6	9	12	0	26	28
sme-miR-124d*	0	4	1	0	0	3
sme-miR-124e	5	35	11	0	59	106
sme-miR-124e*	1	2	1	0	3	10
sme-miR-125a	6	91	30	27	3,267	4,737
sme-miR-125a*	13	543	262	0	1,719	2,361
sme-miR-125b	52	168	85	0	684	957
sme-miR-125b*	0	0	2	0	14	21
sme-miR-13	339	189	114	19	7,002	2,270
sme-miR-13*	0	0	0	0	11	8
sme-miR-133	2	73	24	0	70	299
sme-miR-133*	4	89	42	0	10	26
sme-miR-133a	2	11	3	0	43	101
sme-miR-133a*	0	0	0	0	5	6
sme-miR-184	1	14	7	1	566	1,402
sme-miR-184*	2	71	10	0	25	66
sme-miR-190a	0	4	2	103	22,786	34,636
sme-miR-190a*	39	872	462	2	1,995	5,161
sme-miR-190b	0	6	1	0	1656	2774
sme-miR-190b*	53	1,275	622	1	1,207	2,832
sme-miR-1992	39	136	82	0	33	26
sme-miR-1992*	2	19	3	0	63	55
sme-miR-1993	1	24	8	0	2,485	6,678
sme-miR-1993*	0	11	2	0	291	794
sme-miR-1a	5	156	81	27	92,297	196,424
sme-miR-1a*	1	186	80	0	11	18
sme-miR-1b	149	1,455	799	8	59,781	129,945
sme-miR-1b*	36	1,420	838	0	481	1,016
sme-miR-1c	4	247	152	0	26,275	63,481
sme-miR-1c*	0	9	2	0	138	342
sme-miR-2147a	0	8	10	0	7	9
sme-miR-2147a*	0	0	0	0	38	59
sme-miR-2147b	5	22	7	0	47	79

miRNA genes	454			Solexa		
	Neoblast	Untreated whole-body	Irradiated whole-body	Neoblast	Untreated whole-body	Irradiated whole-body
sme-miR-2147b*	0	0	0	0	11	5
sme-miR-2147c	10	73	49	0	204	294
sme-miR-2147c*	0	3	1	0	17	6
sme-miR-2148	0	22	2	0	105	142
sme-miR-2148*	0	3	0	0	4	4
sme-miR-2149	17	132	49	0	113	94
sme-miR-2149*	15	106	58	0	13	16
sme-miR-2150	0	14	7	1	16	19
sme-miR-2150*	0	5	0	0	9	27
sme-miR-2151	0	66	16	0	5,695	8,353
sme-miR-2151*	0	10	5	0	82	168
sme-miR-2152	120	4	21	6	36	310
sme-miR-2152*	0	0	0	0	0	16
sme-miR-2153	14	143	70	4	272	432
sme-miR-2153*	24	18	19	18	86	204
sme-miR-2154	1	99	33	0	3,002	6,877
sme-miR-2154*	0	2	0	0	12	34
sme-miR-2155	0	0	0	0	3	0
sme-miR-2155*	0	0	0	0	12	14
sme-miR-2156	10	129	51	1	105	243
sme-miR-2156*	0	3	3	0	10	27
sme-miR-2157	0	37	21	0	2,511	6,544
sme-miR-2157*	0	4	0	0	2	8
sme-miR-2158	1	318	195	0	331	831
sme-miR-2158*	0	7	1	0	33	122
sme-miR-2159	32	2,117	1,477	0	49	134
sme-miR-2159*	1	68	28	0	38	88
sme-miR-216	1	42	15	0	577	1,534
sme-miR-216*	0	68	26	0	1,095	1,765
sme-miR-2160	45	24	8	0	35	32
sme-miR-2160*	0	0	0	0	0	0
sme-miR-2161	18	84	39	0	33	85
sme-miR-2161*	0	0	0	0	2	2
sme-miR-2162	73	2,786	1,525	0	27	54
sme-miR-2162*	2	5	2	0	169	263
sme-miR-2163	3	31	17	0	141	246
sme-miR-2163*	0	1	0	0	54	72
sme-miR-2164	1	28	14	0	402	1,291
sme-miR-2164*	0	0	0	0	66	258
sme-miR-2165	0	2	0	0	359	685
sme-miR-2165*	0	1	3	0	54	134
sme-miR-2166	0	0	0	0	3	7
sme-miR-2166*	1	0	0	0	5	3
sme-miR-2167	0	8	4	0	25	57
sme-miR-2167*	0	0	0	0	0	1
sme-miR-2168	0	0	0	0	31	81
sme-miR-2168*	0	1	0	0	11	25
sme-miR-2169	0	0	0	0	17	28
sme-miR-2169*	0	0	0	0	4	12
sme-miR-2170	0	0	0	0	10	14
sme-miR-2170*	0	0	0	0	0	5
sme-miR-2171	0	1	3	0	19	25
sme-miR-2171*	0	0	0	0	0	3
sme-miR-2172	0	1	0	0	4	3
sme-miR-2172*	0	0	0	0	4	1
sme-miR-2173	1	1	0	0	58	90
sme-miR-2173*	0	1	0	0	1	1
sme-miR-2174	0	0	0	0	20	32
sme-miR-2174*	0	0	0	0	0	3
sme-miR-2175	0	0	0	0	1	3
sme-miR-2175*	0	0	0	0	1	1
sme-miR-2176	0	0	0	0	1	3
sme-miR-2176*	0	0	0	0	3	6
sme-miR-2177	0	0	0	0	19	24

miRNA genes	454			Solexa		
	Neoblast	Untreated whole-body	Irradiated whole-body	Neoblast	Untreated whole-body	Irradiated whole-body
sme-miR-2177*	0	1	0	0	0	0
sme-miR-2178	0	1	0	0	587	706
sme-miR-2178*	0	0	0	0	0	2
sme-miR-2179	0	10	3	6	567	673
sme-miR-2179*	0	0	0	0	3	3
sme-miR-2180	3	1	2	0	17	30
sme-miR-2180*	0	0	0	0	0	0
sme-miR-2181	0	1	0	0	16	58
sme-miR-2181*	0	0	0	0	0	0
sme-miR-219	13	295	137	1	1,622	3,761
sme-miR-219*	0	3	5	0	105	204
sme-miR-277a	0	10	3	0	6,284	13,024
sme-miR-277a*	0	1	0	2	100	289
sme-miR-277b	0	0	0	0	1,210	2,311
sme-miR-277b*	10	379	181	0	60	181
sme-miR-277c	3	74	34	0	2,820	5,365
sme-miR-277c*	0	12	12	0	20	38
sme-miR-277d	3	137	75	0	3,238	6,337
sme-miR-277d*	1	305	181	0	260	611
sme-miR-278	32	3,036	1,572	0	2,770	7,126
sme-miR-278*	17	200	84	0	92	213
sme-miR-281	136	1,271	646	1	5,932	12,711
sme-miR-281*	0	22	6	0	62	126
sme-miR-2a-1	987	721	357	0	6,898	11,867
sme-miR-2a-1*	15	237	142	0	96	217
sme-miR-2a-2	987	721	357	0	6,898	11,866
sme-miR-2a-2*	5	176	89	1	916	2,294
sme-miR-2b	1,242	1,732	1,281	0	716	966
sme-miR-2b*	0	6	0	0	1526	3508
sme-miR-2c	57	1,586	1,187	1	2,235	5,270
sme-miR-2c*	0	5	1	15	9,002	18,153
sme-miR-2d	7,222	5,776	3,146	1	402	373
sme-miR-2d*	0	0	0	3	1,276	1,517
sme-miR-315	0	0	0	0	875	1,844
sme-miR-315*	0	0	0	0	2	12
sme-miR-31a	2	28	11	20	832	1,347
sme-miR-31a*	0	0	0	0	126	308
sme-miR-31b	8	157	57	3	654	879
sme-miR-31b*	0	4	1	0	9	19
sme-miR-36	2,198	4,242	2,928	25	2,529	6,318
sme-miR-36*	164	2,564	1,610	0	27	56
sme-miR-36b	320	227	131	12	584	1,148
sme-miR-36b*	0	0	0	0	33	85
sme-miR-36c	111	338	240	11	1,679	4,638
sme-miR-36c*	0	0	0	0	72	194
sme-miR-61	13	210	98	0	8,765	13,810
sme-miR-61*	0	1	2	1	25	87
sme-miR-61b	0	96	32	0	284	531
sme-miR-61b*	3	45	28	0	2,111	2,340
sme-miR-67	0	46	20	0	1,781	3,904
sme-miR-67*	0	5	0	1	137	324
sme-miR-71a-1	290	407	254	1	6,880	9,604
sme-miR-71a-1*	1	76	61	0	11	33
sme-miR-71a-2	289	406	254	3	6,847	9,581
sme-miR-71a-2*	3	264	138	1	218	462
sme-miR-71b	948	857	370	96	14,751	11,550
sme-miR-71b*	10	38	27	1	129	106
sme-miR-71c	279	688	433	5	3,376	6,047
sme-miR-71c*	0	9	6	0	12	36
sme-miR-745	46	392	167	0	4,700	9,652
sme-miR-745*	0	0	0	0	50	112
sme-miR-746	68	604	351	0	770	1427
sme-miR-746*	5	156	65	0	343	734
sme-miR-747	0	37	6	0	2,925	6,589

miRNA genes	454			Solexa		
	Neoblast	Untreated whole-body	Irradiated whole-body	Neoblast	Untreated whole-body	Irradiated whole-body
sme-miR-747*	1	183	102	0	904	1,869
sme-miR-748	3	0	3	0	3,967	9,367
sme-miR-748*	0	0	0	0	5	19
sme-miR-749	11	34	21	0	29	81
sme-miR-749*	0	0	1	0	1	8
sme-miR-750	79	998	445	0	6,127	14,275
sme-miR-750*	0	6	2	0	113	226
sme-miR-751	0	12	1	6	2,121	3,916
sme-miR-751*	0	0	0	0	0	0
sme-miR-752	157	61	24	52	346	98
sme-miR-752*	2	4	6	7	1,058	1,297
sme-miR-753	0	3	0	3	429	467
sme-miR-753*	3	11	8	11	288	407
sme-miR-753b	0	8	1	2	217	223
sme-miR-753b*	52	119	52	11	295	433
sme-miR-754	0	23	7	0	14	64
sme-miR-754*	0	0	0	0	8	21
sme-miR-754b-1	6	134	44	2	205	469
sme-miR-754b-1*	0	0	0	0	4	3
sme-miR-754c	6	108	33	1	180	433
sme-miR-754c*	0	0	0	0	8	22
sme-miR-755	4	388	169	0	665	1,554
sme-miR-755*	3	356	164	0	2,351	5,413
sme-miR-756	582	787	398	1,802	16,520	18,599
sme-miR-756*	0	2	3	0	64	154
sme-miR-79	1,671	4,093	2,615	1	781	1,115
sme-miR-79*	0	4	0	0	582	693
sme-miR-7a	1	5	1	0	149	204
sme-miR-7a*	0	0	0	0	1	9
sme-miR-7b	49	170	64	0	1,163	1,521
sme-miR-7b*	0	0	0	0	8	9
sme-miR-7c	89	263	107	1	2,119	3,721
sme-miR-7c*	15	28	11	0	23	30
sme-miR-7d	18	58	41	0	147	132
sme-miR-7d*	0	1	1	0	1	3
sme-miR-8	132	264	130	0	453	900
sme-miR-8*	2	7	3	0	42	87
sme-miR-87a	83	860	550	0	58	96
sme-miR-87a*	3	46	34	0	135	340
sme-miR-87b	6	91	27	0	1,000	2,402
sme-miR-87b*	7	5	4	1	344	629
sme-miR-87c	5	158	111	0	432	826
sme-miR-87c*	3	19	13	0	24	55
sme-miR-87d	7	24	4	3	124	278
sme-miR-87d*	1	6	1	0	84	150
sme-miR-8b	37	283	116	0	1,459	3,139
sme-miR-8b*	0	0	0	0	5	8
sme-miR-92	1	15	2	0	327	717
sme-miR-92*	1	307	197	0	11	30
sme-miR-96a	0	19	11	4	3,191	6,175
sme-miR-96a*	0	0	0	0	21	50
sme-miR-96b	0	16	10	2	3,143	5,970
sme-miR-96b*	0	0	2	0	0	1
sme-miR-9a	0	15	6	2	2,015	4,998
sme-miR-9a*	1	1	2	0	24	52
sme-miR-9b	0	20	5	0	606	1,143
sme-miR-9b*	0	2	1	0	45	101
sme-putative-753.1	1	8	6	1	15	40
sme-putative-753.1*	1	6	10	5	366	604
sme-putative-753.2	5	17	21	5	373	600
sme-putative-753.2*	52	119	52	11	297	434
sme-putative-753.3	2	99	55	0	1,007	2,010
sme-putative-753.3*	0	0	0	2	6	16
sme-putative-753.4	2	99	55	0	1,007	2,010

miRNA genes	454			Solexa		
	Neoblast	Untreated whole-body	Irradiated whole-body	Neoblast	Untreated whole-body	Irradiated whole-body
sme-putative-753.4*	52	119	51	11	280	421
sme-putative-753.5	0	12	10	2	1,072	1,860
sme-putative-753.5*	52	119	51	11	290	423
sme-putative-754.1	0	51	17	0	4	14
sme-putative-754.1*	0	0	0	0	6	18
sme-putative-754.2	6	134	44	2	205	469
sme-putative-754.2*	0	0	0	0	9	22
sme-putative-754.3	6	112	33	1	88	161
sme-putative-754.3*	0	0	1	0	8	22

Table S2. Analysis of long (>25 nt) reads mapping to intergenic regions, exons of protein coding genes, exons of conserved protein coding genes, introns of protein coding genes, introns of conserved protein coding genes, and our annotated piRNA clusters

Region	Long, uniquely mapping reads per mega base
Intergenic	200 ± 10
Exons, sense	350 ± 10
Exons, antisense	90 ± 10
Exons from homolog genes, sense	390 ± 20
Exons from homolog genes, antisense	30 ± 10
Introns, sense	210 ± 10
Introns, antisense	130 ± 10
Introns from homolog genes, sense	190 ± 40
Introns from homolog genes, antisense	70 ± 10
piRNA clusters	16300 ± 700

All counts were normalized to the length of the type of annotation summed over the genome. Standard errors were calculated by randomly splitting the mappings into 5 sets and repeating the analysis for each set.

Table S3. Total expression of miRNAs and piRNAs normalized to 3 miRNAs that were constant in the 3 samples according to qPCR (See *SI Methods of SI Text*)

miRNA	miRNAs			piRNAs		
	Neoblast	Untreated	Irradiated	Neoblast	Untreated	Irradiated
miR-71c	0.9	1	0.9	46	1	0.25
miR-36	0.7	1	0.8	7.1	1	0.19
miR-36c	1.1	1	0.8	10	1	0.17

The miRNA and piRNA expression of the untreated sample was set to 1, and the other expression levels were scaled accordingly. The large variance of piRNA expression in the neoblast sample is likely an effect of the low read counts for the miRNAs used for normalization in this sample.

Table S4. piRNA transposon association

Repeat class	Total genome coverage of repeat, Mb	Total genome coverage of repeat, fraction	Fraction of piRNAs in the untreated sample mapping to repeat type	Fold enrichment, fraction of piRNA coverage/fraction of genome coverage
DNA_TcMar	12.16643208	0.014065239	0.026605987	1.892
DNA_hAT	9.772936599	0.011298193	0.018968193	1.679
LINE_Penelope	16.63934215	0.019236234	0.026799082	1.393
LINE_R2	23.6842331	0.027380616	0.02754767	1.006
Low_complexity	21.26549164	0.024584383	0.019532837	0.795
LTR_Gypsy	116.9148185	0.13516164	0.106542	0.788
DNA_Maverick	47.64749046	0.055083804	0.034961253	0.635
Simple_repeat	14.28672666	0.016516447	0.009141375	0.553
DNA_PiggyBac	40.20635564	0.046481336	0.023200735	0.499
DNA	2.020804264	0.00233619	0.001091767	0.468
Unknown	4.755393898	0.005497565	0.002202752	0.401

The piRNA enrichment is calculated as the transposon piRNA coverage divided the transposon genome coverage. Only major transposon classes are shown.

Table S5. Location and intensities of the 119 planarian piRNA clusters

Genome contig	Begin position of cluster	End position of cluster	10 nt overlap intensity of long, uniquely mapping piRNAs	No. of long piRNAs mapping uniquely to the genome plus strand of the cluster	No. of long piRNAs mapping uniquely to the genome minus strand of the cluster	10 nt overlap intensity of mapped piRNAs	No. of piRNAs mapping to the genome plus strand of the cluster	No. of piRNAs mapping to the genome minus strand of the cluster
v31.000000	290000	300000	4.41	1	579	4.41	4.44	737.33
v31.000001	100000	110000	2	100	5	9.69	151	17.57
v31.000016	70000	80000	6.45	14	170	8.32	22.9	245.48
v31.000056	100000	110000	1	116	1	1	176	2.87
v31.000077	230000	240000	2	3	187	2	5.99	259.67
v31.000111	60000	70000	1	1	1003	1	1.8	1144.28
v31.000132	80000	90000	2.41	110	4	9.44	172	13.96
v31.000132	100000	110000	1.41	99	3	21.6	215	6.51
v31.000144	170000	180000	8.59	482	3	40.9	602	4.11
v31.000169	130000	140000	136.14	1435	50	204	1782	66.76
v31.000169	170000	180000	10.14	431	2	15.1	556	6.99
v31.000179	110000	120000	1	3	231	1.57	6.02	317.02
v31.000182	150000	160000	79.54	47	104	168	107	167.01
v31.000200	70000	80000	4	206	2	6.28	238	6.93
v31.000200	190000	200000	7	277	2	7	346	2.27
v31.000205	120000	130000	7.65	2	179	9.49	3.64	230.62
v31.000221	30000	40000	4.41	1	274	4.55	1.72	346.5
v31.000221	40000	50000	3.73	3	704	3.94	4.97	815.2
v31.000254	30000	40000	21.48	186	1	21.5	235	2.14
v31.000265	70000	80000	1	98	3	1	115	3.8
v31.000265	170000	180000	1	5	729	3.62	8.37	928.36
v31.000265	180000	190000	5.82	2	314	6.39	2.02	389.92
v31.000307	10000	20000	3	4	96	3.45	11.5	110.99
v31.000333	30000	40000	3.41	224	1	4.34	327	1.7
v31.000338	60000	70000	1	2	154	2	2.3	191.61
v31.000338	100000	110000	3	233	6	13.3	312	7.58
v31.000342	100000	110000	21.11	8	588	27.6	23.3	728.18
v31.000342	110000	120000	2.41	4	229	5.82	13.5	427.51
v31.000355	130000	140000	4.82	4	106	11.2	8.71	147.4
v31.000359	0	10000	2.41	1	121	2.41	3.04	146.73
v31.000361	100000	110000	1	3	139	2.5	5.41	176.2
v31.000465	70000	80000	2	272	5	6.6	442	12.37
v31.000466	40000	50000	9.07	165	3	12.7	199	3.57
v31.000466	50000	60000	12.64	122	55	65.2	190	176.48
v31.000511	90000	100000	2	446	1	2	539	1.77
v31.000521	70000	80000	1	2	141	1.98	2.27	220.07
v31.000521	80000	90000	2	4	182	2	5.04	233.27
v31.000532	20000	30000	5	1	117	5.32	3.94	160.16
v31.000554	60000	70000	28.17	2	134	32.4	3.65	169.11
v31.000558	110000	120000	65.36	13	235	91.1	26.4	287.6
v31.000558	140000	147967	4.41	6	199	5.04	11.1	263.91
v31.000564	90000	100000	1	3	413	8.87	10	548.17
v31.000590	110000	120000	6.41	181	4	9.4	341	11.01
v31.000617	20000	30000	1	125	3	4.15	170	3.77
v31.000652	120000	130000	2.41	106	2	24.5	168	8.84
v31.000672	80000	90000	12	4	202	12.9	5.22	318.52
v31.000741	50000	60000	1	2	229	5.99	2.71	352.49
v31.000751	50000	60000	283.67	159	48	405	207	76.16
v31.000753	130000	139189	1	2	112	2.7	5.04	138.84
v31.000866	20000	30000	1.41	221	3	1.97	277	5.45
v31.000886	60000	70000	14.38	1	234	25.8	2.53	305.75
v31.000900	100000	110000	1	1	376	85.1	15.1	493.21
v31.000911	0	10000	1	98	2	1	162	3.74
v31.000918	20000	30000	5.82	224	1	7.97	352	2.51
v31.000995	70000	80000	2	1	348	2.14	2.76	424.22
v31.001066	90000	97060	9.23	3	227	14.1	3.06	300.34

Genome contig	Begin position of cluster	End position of cluster	10 nt overlap intensity of long, uniquely mapping piRNAs	No. of long piRNAs mapping uniquely to the genome plus strand of the cluster	No. of long piRNAs mapping uniquely to the genome minus strand of the cluster	10 nt overlap intensity of mapped piRNAs	No. of piRNAs mapping to the genome plus strand of the cluster	No. of piRNAs mapping to the genome minus strand of the cluster
v31.001076	40000	49260	2	2	320	222	7.67	2934.65
v31.001093	30000	40000	1	108	4	2.49	145	6.54
v31.001191	30000	40000	24.86	4	156	33.8	7.88	203.88
v31.001204	30000	40000	34.21	221	2	41.2	284	3.67
v31.001206	50000	60000	7.18	3	443	16.1	17	518.77
v31.001207	30000	40000	1	5	147	3.35	7.09	184.07
v31.001207	40000	50000	24.33	1	298	26.9	1.45	373.46
v31.001225	40000	50000	1	311	2	1	422	3.89
v31.001232	0	10000	1	246	2	2.67	324	7.11
v31.001345	20000	30000	1.41	276	4	3.54	371	5.09
v31.001374	60000	70000	1	3	633	1.37	4.89	862.47
v31.001417	40000	50000	3	135	2	3.02	183	2.17
v31.001417	50000	60000	2.41	142	2	3.41	183	4.84
v31.001551	20000	30000	4	148	1	8	201	1.04
v31.001568	70000	80000	2.41	1	130	7.69	2.63	186.21
v31.001575	40000	50000	18.37	141	103	44.1	211	154.43
v31.001576	30000	40000	13.59	346	2	22.2	438	6.15
v31.001621	40000	50000	1	219	3	1	298	6.32
v31.001801	70000	80000	2.41	2	2347	9.53	3.56	2603.73
v31.001826	40000	50000	22.87	4	175	45.5	6.33	222.99
v31.001892	40000	50000	12.42	542	22	42.3	698	33
v31.001892	50000	60000	5	992	2	19.5	1253	6.07
v31.001892	60000	70000	9.38	303	4	14.6	399	8.37
v31.001892	70000	78621	1	186	1	5.22	241	3.46
v31.001973	20000	30000	4.41	3	103	17.8	6.74	134.18
v31.002051	0	10000	58.25	2	319	103	3.73	357.35
v31.002093	10000	20000	2	3	418	7.74	4.35	476.96
v31.002339	20000	30000	1	2	246	4.32	6.91	374.26
v31.002365	30000	40000	1.41	221	3	5.33	307	4.93
v31.002415	30000	40000	2.41	4	236	13.6	5.11	322.24
v31.002528	10000	20000	36.95	143	12	59.8	181	14.87
v31.002537	20000	30000	25.28	2	668	71.7	5.42	806.57
v31.002537	30000	40000	2	3	101	2	4.06	139.37
v31.002549	50000	60000	4	458	3	4.33	574	3.98
v31.002684	10000	20000	2	125	1	7.04	252	2.04
v31.002688	20000	30000	3.41	223	1	5.27	285	4.68
v31.002788	20000	30000	2	222	1	2.28	301	3.06
v31.002788	30000	40000	1	234	1	1.71	324	3.5
v31.002965	40000	50000	118.07	2	596	137	2.27	677.09
v31.003034	10000	20000	63.02	5	199	107	5.31	270.16
v31.003118	20000	30000	2	1	374	3.61	3.77	487.43
v31.003208	60000	70000	1	104	3	2.2	198	7.46
v31.003212	20000	30000	12.29	246	2	13.6	323	5.97
v31.003763	20000	30000	7.41	2	209	13	4.17	314.47
v31.004482	10000	20000	2.73	1	331	2.73	1.86	436.82
v31.005110	0	10000	1	4	133	4.97	9.89	207.91
v31.005212	30000	40000	69.35	38	98	139	59.2	128.93
v31.005332	30000	40000	69.94	103	118	105	166	165.17
v31.005594	30000	40000	2	4	149	16.5	5.35	371.11
v31.005657	10000	20000	6.82	3	172	7.82	8.32	222.23
v31.005856	0	10000	2	93	19	4.42	125	28.2
v31.005979	10000	20000	9.73	2	125	23.7	3.04	165.67
v31.006652	20000	30000	35.48	273	2	80.4	652	7.87
v31.006721	10000	20000	4	33	73	21.7	65.6	158.35
v31.006827	0	10000	4	6	101	4	7.13	135.39
v31.006841	10000	20000	5.14	321	1	5.14	407	2.21
v31.007165	10000	20000	1	160	4	4.65	201	5.9

Genome contig	Begin position of cluster	End position of cluster	10 nt overlap intensity of long, uniquely mapping piRNAs	No. of long piRNAs mapping uniquely to the genome plus strand of the cluster	No. of long piRNAs mapping uniquely to the genome minus strand of the cluster	10 nt overlap intensity of mapped piRNAs	No. of piRNAs mapping to the genome plus strand of the cluster	No. of piRNAs mapping to the genome minus strand of the cluster
v31.007275	10000	20000	4.82	110	3	9.32	159	3.84
v31.008899	0	10000	1	1	153	1.96	2.38	884.35
v31.008899	10000	20000	1	2	236	1	2.08	360.35
v31.009965	0	10000	1	1	203	1	5.3	259.66
v31.014194	0	10000	39.47	50	93	66.2	87.7	278.34
v31.020292	10000	17329	1	1	140	2.26	2.14	198.36

The positions of the clusters were inferred from the Solexa sequencing of untreated planarians. All numbers in this table derive from this dataset. The first column is the id of the genome contig. The second column is the genomic start position of the cluster bin on the contig. The third column is the genomic end position of the cluster bin on the contig. The fourth to ninth columns indicate the intensity of read mappings and ten nucleotide overlapping events (*Methods*).

Table S6. Overview of the novel planarian miRNAs

Novel miRNA	Mature sequence	Precursor sequence	Genomic location of interest
sme-let-7d	AGAGGUAGUGAUUCAAAAAGUU	CUUCCUAUAUUCAUUUUACUAGAGGUAGUGAUUCAAAAAGUU- AAUUUAAACAUUUUGACUUUUUGAAUUAUAUCUUUGAUAA- AUGAUUGAAAGACAUCA	
sme-miR-10a	AACCCUGUAGAUCGAGUUAGAU	UAAUUUGUUUCCUUGAUUAUAAACCCUGUAGAUCGAGUUAGA- UGGUUUUCCAAUUCGAAUUCUCGGGGAUUUAUUAUUAUGA- GAUUUUCUUCU	
sme-miR-1175	UGAGAUUCAACUCCUCCUACU	UAUUAAAAUUCUAAAAUGAGUGGAGAUGUUGAAAUUCAAAAA- AAUAAUUUCGUUUUUUUUGAGAUUCAACUCCUCCUACUAA- UUUGGGAUUUCAAACU	
sme-miR-124d	UAAGGCACGCGUAAGUGGGU	UUGGAAUUGUUUUAAUAAAACAUUUCAAGCAGCCUUAAU- UAGAAUUCAAUUAAGGCACGCGUAAGUGGGUUGUUGAAA- UUCCUAUCAUCU	
sme-miR-124e	UAAGGCACGCGUGAAUGCCA	UUCAUAAAAUUAUUCUACUGCCAUUCUCAGUUGGAGUCUUGA- UAUGAUCUAUUAAAGGCACGCGUGAAUGCCAAGGAAUUUU- AUUCUCUUCU	clusters with sme-mir-8b
sme-miR-133a	UUGGUCCCCGUAACCAGCUGU	AAUCGCAGUAUAUUUAUAGCAGCUGUUGACGAAGUAUCAAAA- UAGUUAAAUGAUGAUUAUUUUUUUUGGUCCCCGUAACC- AGCUGUUUAUUUGUAUUAUAAACUCC	
sme-miR-1992	UCAGCAGUUGUUCUUGAC	UUAUGAAAAAAGAAUUUGUCUUGAACACUCGUUAUGAUGA- AAAAAUGUCAUCAGCAGUUGUCCAUUGACAAGUUUAUU- UCAUUGAUAU	
sme-miR-1993	UAUUUAGCUGUUAUUAUGA	UUAACCUUCGAUUGUAUUGAUGAAUCAACAGUAUAAAAAC- GGAGUACAACAAUUAUUCGUUAUUUUGCUGUUUAUCAUGAG- UUACUAUGGAUUUAUCGUCG	
sme-miR-2147a	CGGAAGACUCGCACGUGAC	UCUUCUUUGGUAUGCCAACGGCGGAAGACUCGCACGUGACAUU- GCUAAUUUUUCCAUUUCACUGCGAGUGUCCCGCGUUGA- UCCCAAUUCUCAUCA	
sme-miR-2147b	CGGAAAACUCGCACGUG	CCUUCUUUGGAUACUAACGGCGGAAAACUCGCACGUGUCCUC- GUC AACUUCACGAUUUCACGGCGAGUGUCCACGUAUU- UCCAAUUCUCGACA	
sme-miR-2147c	CGGAAAACUCGCUCGUGCCAUCGU	UUGUUUUGCUGUAUAACGGCGGAAAACUCGCUCGUGCCAUC- GUCGUCUUCACGAUGUCACGGCAGGUGUCCACGUAUU- CCCAAUUUCCUCA	close sense to unknown gene
sme-miR-2148	AGAAAUUCUGUGGUCUUGAUU	GUAAGUAACCAGUUUAUCAGAGAAAUCUGUGGUCUUGAUUG- UAAAUGAUUAUUAUCUGGCCACAAAUUUUUUUAUUA- ACGUUUGAACUUCA	clusters with sme-mir-2177
sme-miR-2149	CGCCAAUGACAAACUGUUGAU	GCAGAAAGAUCAAUUGAGUACCGCCAAUGACAAACUGUUGAUG- AAGACUUUGUCACAAUUAUCAGCAGUUGUCCAUUGACGUU- AUUUACCUUCGUUUUCAUCG	
sme-miR-2150	CGGUUACGUGAUUAUAGGGG	UCAAAUCGGACUUCUCUAUUCGGUUAUCGUGAUUAUAGGGGC- AGCGGCUUCGUCUGUGGUAACUGUCACUAGCAAGAAAGU- UCCUUAUGUAGUCAUGUGACCUCAUGACCGAUUGCAAUUU- CUUC	
sme-miR-2151	GAUUGCACUCAAUUAGGUCAGAU	UGCUUAAAGAGAACUCUUUACAGAUCAUGUUAAGUGGAAUUUG- AUAAACAGAUUGCACUCAAUUAGGUCAGAUUAGCUUUCUCU- CAACAGCA	
sme-miR-2152	GGGUUCGAAGUAUGUCUCUCUUU	CUUAUUCUCAAAAUUUAAAUGGGUUCGAAGUAUGUCUCUCUU- UAUUUGGAGAUUAUAUCGAAUACGAAUGACUAGUGAGCCA- UUUUU	
sme-miR-2153	UAGGCAUAGUCUGUUGGUUACU	UAAAAUACGGAUUUUGAUUAGGUAGGCAUAGUCUGUUGGUUA- CUUCUAUGAAAUUGAAUUGAUCAAUAAUACCCUUGAC- CAUGGACGCGACCCUACCUUUUAUUGAAUGAAAUAUUUCG	
sme-miR-2154	UCAGCUGUACAAUUGCAUUGUGU	UUCGAGUGAUUAUUAAGAAUUUCAGCUGUACAAUUGGCAUUGU- GUAUGAUAAAUGAAUUAUUAACAACAAGUCUUUGUAUAGC- UUUAUUUUUUUAUCACUAAUCCACC	
sme-miR-2155	GACACUGUUUUACACUUACCCGA	UAUUUGAUGUAAAAGUGCAUCAGGAUAAGUGUAUAGCAGUGUU- AAUUUGACACUGUUUUACACUUACCCGAUGCUCAGAGAAA- UUUGAUG	
sme-miR-2156	UCUUACGGCCCCUAAACUUUUA	UUUUUCAAGUCAUGAAAUAUAAAAGUUUUGGGUCAUAACAUA- AAUAAUUUUUAUUAUCUUACGGCCCCUAAACUUUUAUUU- UCAAGAUUCUACAGCA	

Novel miRNA	Mature sequence	Precursor sequence	Genomic location of interest
sme-miR-2157	UGAGUAUUGCAUCAAGAACCGA	UUAAAGGUGCAGUCAAAUUUUGAGUAUUGCAUCAAGAACCGA-AUGUUAAUAUCAGUUUUUGAUGAAUUACUUAAAUAAGCU-CCUCUAAUCUCUU	clusters with sme-mir-216
sme-miR-2158	UGAGUAUUUUUUCGUAUACCGA	GGAAAGUAUUUUAAUUUUUGAGUAUUUUUUCGUAUACCGA-ACAGAUCaucGUUGACUUUCGGUAACGAAGAAUACUUGGA-AUUGAGAAAUUUAUUCGUCG	clusters with sme-miR-747
sme-miR-2159	UGCCUUUUUUUGAGUAGC	AAUGCAAAUGAAUUCAAAACUGCCUUUUUUUGAGUAGCUGU-CCGCAGACAGGUGGAGCUGCCAAAUAAGGGUGAUUUGGA-AUUCAUUCAUCGUA	
sme-miR-216	CAAUCUCAGCCUGUUAAUAGGAGUU	CCUGUCAUGAUUUAGCAAGCAAUCUCAGCCUGUUAAUAGGAG-UUUGGAAAUGUUAAAUCUCCUAUAACGUCUGAUGAUUA-CUUGUCAAAUCAUUUUACCAA	clusters with sme-mir-2157
sme-miR-2160	UGGCGCUUAUGUGUAGAACCGG	AAAAUCUUUGUGAUUUAAAUAUGGCGCUUAUGUGUAGAACCGG-UUGUACUAUAAUUUUAAACUGGUUUUUCUGUAAGAGCCC-AAUAGUAUCACAAAAUCAUC	close to SMAD gene
sme-miR-2161	UGUGCGUAGUAAUAGAGGUUUC	UUUUCUUUGUCUGUAUAGUAUCUUUUUUUUAUCGUACAAA-AUGCUUGCUUAGGUUGACAUUUUGUGCGUAGUAAUAGAGG-UAUCAUAUAGUCAUUUAUCGUC	
sme-miR-2162	UGUGCUUAAUUUGUAUAUUGC	UGGCGUAGUCUAUGGUGUAUUGUGCUUAAUUUGUAUAUUGCAC-UGUUAUCUUUUUGUAUUUGCAAAUAUUCACAAUUUGACC-AAGCUAAACAUC	
sme-miR-2163	UUGCAUAGUCUAUUAAGUUGGU	AUUACGAGAUUUUAUUUUAUUAACUUGAUAGAUUAUUGCAUC-AACGAGAUUUGCUAUUAUUUUUGUUGCAUAGUCUAUUUAGU-UGGUCGAAAUGAUUUUAAUCGUA	
sme-miR-2164	UUGUGCGUGAUUCAAGUAUAAU	CCAUAUUCAGGUAUAAAUAUUAUUUGAUUUCACGUAGAGAU-UGAGAUCUAUCUUGUGCGUGAUUCAAGUAUAAUAAUGUU-CUGACUCUUCUUCU	
sme-miR-2165	UAAUUCGAUUCUUUAGAGUAUU	AAACUUUAUUGAAUCCGAUCAUUCUACAGGAUCGAAUACAGU-UUGUAAAUUUGUAAACUAUCUCUUAACUAUUUCGAUUCU-UUAGAGUAUUUGAUUUCAUUUUUUAUUCGUCG	
sme-miR-2166	UUGGUCACUUGCUUUUUAUUCACUC	AUAUGAAAUCUAUUUUUCUCUAGAAUAAAACAGAUACCAAU-CAUGUUUCAGUUGAAUCUGAUUGGUCACUUGCUUUUAUUCACUCAUAAAUCUAAAUAUAAUAGC	intron of unknown gene
sme-miR-2167	UGUGUUAAGCUGGUCUUUCAGA	UGUGAAUGCAAUUCUAUCUUUGAAAGACAAGUCUUUAUACAUU-CUUAGUGUCAAAACAUCCAAGUGUGUUAAGCUGGUCUUUCA-GAGCAUGAAUUCGUUAAUCGUC	close antisense to unknown gene
sme-miR-2168	AUAUUCGUUAAGGUUGUAAC	AUGCCAGAAAUUCUGAUGCCAUUUCGUUAAAGGUUGUAACCA-GACACUUUGGUCACAACCUUUGACGAAUGAGGAGUCAUUU-UUGGUAAAUCAU	
sme-miR-2169	AACUUUGAAAUUCGAUCUGAU	GAAUUUUUAUCACUCUAACAACUUUGAAAUUCGAUCUGAUUA-AAAUAUUAUAAAGCUCGAUUAUUAAAGUGGUUUUCGUGA-UAUUUUUCGUC	close sense to proliferation-associated 2G4 gene
sme-miR-2170	ACAGUGAAAUUUGUAGAGA	AUAAAUGGCAUUAUUAUUUUCUCUACUAAAUUUCACUAUGAAU-UUAAGGUUAUUCACAGUGAAAUUUUGUAGAGAAAUAUAAU-AAAUUGCUUGU	
sme-miR-2171	GUGAUGGAAAUCGCUAUUUCA	GAAAACGCAACAGUACAAAUGUGAUGGAAAUCGCUAUUUCAA-AUGCUCUUUGAGAUUAUGCAGUGGCCGUUCAUGAUGUAA-GGCAUAAUAGAAA	
sme-miR-2172	UACAUGUAUAGUAUUUUUGCCU	AAUAAUUUUCCAUGAUUUUGGAAAUAUAGACUAUGCAUGGGA-CAUUAGUAGAGCUUGUACAUGUAUAGUAUUUUUUGCCUGU-CAUUGGAUUUAUCAGCGA	
sme-miR-2173	UACAUGUACAUUAAGUUGAAUUC	ACAAUUCUAGUAUCAAUGGAAAACAACUUGUAUAUGCAUACG-UAUAGAAAGAAAACAUAUACAUGUACAUAUAAAGUUGAAU-UCAUUGUUUAUAAAUCAUCCGA	
sme-miR-2174	AUUUCGCUGUGAGUGUUC	UCUUUGGAACGUUAAACUUCGAAAACCCGCAUUGCGUUUAUG-UCAACCCUACAAUUUCGUCUGAGUGUUCUCCAUUGUAGCU-CCCAUUUUCGA	close sense to thimet oligopeptidase gene
sme-miR-2175	UACUGAAUGUCUUUUUGCAAAUUGA	CUAUUGGUAGCCAUUGAUGUUUUUGCAUAAAUAUUCAGUAA-AAUGACAUUACUAGAAUUUUUUUUUACUGAAUGUCUUU-UUGCAAAUUGACAAUGCUACUUGGCCCAUUA	partly overlapping with gene model, but mature, loop and star represented
sme-miR-2176	AGAACAUUCUGAUUCACAA	UGAUCAAAAGCAAAACCUUUGGAAUUCGGAUUGUUCUUCAGU-UAAGAACAUUCUGAUUCACAAGGUUUUGCUUCUUAUCACA	

Novel miRNA	Mature sequence	Precursor sequence	Genomic location of interest
sme-miR-2177	AAAUGCCCAGUGAAUUUCUCGGU	AAAAUCAUUGCACAUGAUACAAGAAUUCAUUGGUUAAUUU- CAUGAUUAUGAAAAUGCCCAGUGAAUUUCUCGGUAGAUGA- ACAAUUAUUCAUUU	clusters with sme-mir-2148, partly overlapping with gene model
sme-miR-2178	UAAUGACGAAAUGUCUCA	UACGAGACAUUUCACAUUGCAACAUUUCACAUUAUAGCAA- UUCACUAAUGCACAUCUUAUAAUGACGAAAUGUCUCAUG- AUGAAAUGUCUCAUGA	
sme-miR-2179	AGACUAUAGAGAUUUUUGCUAU	CAUACUAAGUCUUAUUUGUAUUGCAAAAAUUAUUUAUUUAAAC- UCAUUUCUCUAAAUGAGACUAUAGAGAUUUUUGCUAUGCA- UUAGGCUGGAGCCGCUA	
sme-miR-2180	UGGAAUGUGAUAAAGGUGCUU	AUAUAUAUAUAUAUAUACCAACCCUCAUCCAUACUCAUGGA- AAAUGGAAUGUGAUAAAGGUGCUUGAAUUAUACUUGAAAU- AUUG	
sme-miR-2181	UAUGCUGUAAUUAAGCGAUUGGUU	UCAACUAUUCGAUUUUGUCAUAUGCUGUUAUUUAGCGAUUGG- UUUGAAAGAGUUUCUUUAACCAUACUAAUUCACAGCACU- UGUUUAUAUCUGUGAGCCAUA	
sme-miR-315	UUUUGAUUGUUGCUCUGAGAGUU	GUUGAGCGAGGCUUAUAGAAUUUUGAUUUGUUGCUCUGAGAGU- UAAUAUAAUUCAAUGAUAAACUGUCUAAACAACCAUCAAAU- UUCAAAGCGAUGCUUGUCAUCG	
sme-miR-36b	UCACCGGGUAGACAUUAAUCAUG	UUUUUUAACAGUCUAAACUCUGGAUUGAUUUAUUCGGUAUGA- UCUAGAAUAAAAUUAUCACCGGGUAGACAUUAAUCAUGC- AGUUAGAGUCUGUAGUCCU	clusters with let-7b
sme-miR-36c	UCACCGGGUAGACAUUCAU	AAUUUCAACAUAUUUAGCGAUGAUUGUCCAACUGGUUUUGU- GUCGAGUUGAAAAUGCAUCACCGGGUAGACAUUCAUUCU- CUAAAUUUAUCGUCAAUUCU	clusters with miR-36
sme-miR-61b	UGACUAGAAUGUUCACCUUCUUU	CAAAGCGGGCAUUACACAGAAGAUUGUUGCUGUUCUAGAUUAC- AUGGAUAUAUGUGACUAGAAUGUUCACCUUCUUUAGUAGA- AUCGCGAUCUUCU	
sme-miR-753b	AAGCUUGGAUUGUGAUCUCA	UUUUAAUAAAGUAUUAUUAAAAGCUUGGAUUGUGAUCUCAUA- UAUUUAUGAGAUCAUUAUUCAGCUCUUAUAAUAAUUCUUU- UCAUCAAC	intron of R3H domain containing protein
sme-miR-754b-1	GUUGCUUGGGGGUAUUACU	GUUUUAUCAUCCACCCAGCAUGUUGCUUGGGGGUAUUACUAUA- UUUAUUAAUUAUUUUUAUCAUCAAGCAAUAUCAGAGGUG- AAAUUAUCAUCU	
sme-miR-754c	GUUGCUUGGGGGUAUUAU	ACGAUGCAUUCACCCAGCAUGUUGCUUGGGGGUAUUUAUUA- UUUAUUGAUUAUGUUUAUCUUAAGCAAUAUCAGAGGUG- GAAUAUUCAACA	
sme-miR-7d	UGGAAGACUAGUAAUUUUGUUGU	AAAAACUAUAAAAACAUCUUGGAAGACUAGUAAUUUUGUUG- UAUGCGAAUUUUUAUCAGACAUUCAGUUUGAGAGGAUUUA- CAACAUUAUUUCUGUUUCCAAGAAACUUAUAGUCAAUUC- AACG	
sme-miR-87c	AUGAGCAAAUUAUCAAUUGACU	GUUCUCGGCUCGUGUCGACUCAAUUGAUAAUGGGCCCCAGC- CAUUCAGGGCAAUGAUGAGCAAUUAUCAAUUGACUUCU- CAUGGCCAUUGUCAUCU	
sme-miR-87d	GUGAGCAAAGUUUAAGACAUUC	UUACAUUGUUUAGAAUUUAUUAUGUCUUUAUUUUGCUAUUA- UCAUUGUUUCAUUGAAAUGGUGAGCAAAGUUUAAGAC- AUU- CAUAAUUUGAAAUUUCUUCU	
sme-miR-8b	UAAUACUGUCAGGUAAGAAUACU	UGCAUUCAUUCUAAUAAUUUGCUUCUUAUCUUGAUGGUAAGAG- ACAGAUUUUUGUUUAUACUGUCAGGUAAGAAUACU- GACUAAUAGAAUUAUCUUCG	clusters with sme-mir-124e
sme-miR-96a	UUUGGCACUUAAGGAAUUGUCACU	CUUCAUUUGAGUAUAUUCGUUUUGGCACUUAAGGAAUUGUCA- CUAGUGUUUUUUAAAGUUUCGGUGACAAUACUAAAGAGU- CAAGCGUUUACAUCUGAUUCGUUCA	intron of unknown gene
sme-miR-96b	UUUGGCACUUAAGGAAUCGUCAC	UAUCAAAACAGUUGUCUGAAUUUUGGCACUUAAGGAAUCGUCA- CCAGUUGCAUUGAUUAUUGGACAUUUUCUAAAGUGUCUUAUA- UCAGAGAUUGGUUAUCAUCU	
sme-miR-9a	UCUUUGGUUUUCUAGCUGUAUGAU	UUGUUUAAUUGACUAUUAUGGUCUUUGGUUUUCUAGCUGUAUG- AUUGUAAAAUUUGUUGAAUUCACACACUAGAUUACCAAUU- UCAUAUAUUAUUGGAUCAUCU	
sme-miR-9b	UCUUUGGUUGUUUAGCUUAUUGA	ACAAAUGUCAAAUCAAGAUAUCUUUGGUUGUUUAGCUUAUUG- AAUGUCUAGGCAUAUACUGCAUAAUCAAGUUGUCUG- AUUUGAGUAAGCUUC	

Novel miRNA	Mature sequence	Precursor sequence	Genomic location of interest
sme-putative-753.1	AGGCUUGAAUUGUGAUCUCA	UUUUUAUAAAAGCAUUAUUUAAGGCUUG- AAUUGUGAUCUCAUAUUAUUUUGAGAUC- AUUGUUCAAGCUCUAAA-UAAUACUUUUCAUCAUUG	
sme-putative-753.2	AGGCUUGAAUUGUGAUCUCC	UUUUAAAUAAGUAUAUUUAAGGCUUGAAUUGUGAUCUCCUA- UAUUUAUGAGA- UCAUUAUUCAGCUCUAAAUAUUAUUU- CAUCAACG	
sme-putative-753.3	AGGGUUUGGAUUGUGAUCUC	UUUUUAUAAAAGUAUAUUUAAGGGUUUGGAUUGUGAUCUCAU- AUUUUAUUGAGAUCAUUAUCCAAGCUCUAAAUAAGGAAU- UAUGCCAAUU	
sme-putative-753.4	AGGGUUUGGAUUGUGAUCUC	UUUUUAUAAAAGUAUAUUUAAGGGUUUGGAUUGUGAUCUCAU- AUUUUAUUGAGAUCAUUAUCCAAGCUCUAAAUAUAC- UUC- AUUAACGUGU	
sme-putative-753.5	GAGCUUGGAUUGUGAUCUU	UUUAUUAAAAGUAUAUUUAAGAGCUUGGAUUGUGAUCUUGUA- UAUUUAUUGAGAUCAUUAUCCAAGCUCUAAAUAUACUUU- CAUCAUCA	
sme-putative-754.1	GUUGCUGGGGUUUACUA	AUUUGUCAUCCACCCAGCAUGUUGCUUGGGGUUUACUAUAU- UUUUUAUUAAGUUUUAUCUUCAAGCAAUAUCGAGGUGG- AAUAUUCACAA	
sme-putative-754.2	GUUGCUGGGGUUUACUAU	AUUUAGCAUCCACGCAGCAUGUUGCUUGGGGUUUACUAUA- UUUAUUAAAUAAGUUUUAUCUUCAAGCAAUAUCAGAGGUG- GAAUCAUCUUCA	
sme-putative-754.3	GUUGCUGGGGUUUACU	AUUUAACAUCGCCAGCAUGUUGCUAGGGGUUUACUAUAU- CUUAUUAAU- AUAGUUUUAUCUUCAAGCA- AUAUCAGAGGUGGAUCAUCUUCA	

The precursor sequences include 20-nt-long flanks.

Table S7. Fold change of miRNA expression in the untreated, irradiated, and neoplast samples as measured by the 454 and Solexa sequencing

miRNA	454, nb vs. un	454, nb vs ir	454, un vs. ir	solexa, un vs. ir
sme-bantam-a	0.52	0.64	1.23	1.41
sme-bantam-a*	0.04	0.04	0.96	1.22
sme-bantam-b	0.8	0.83	1.03	1.43
sme-bantam-b*	2.73	1.55	0.57	1.44
sme-bantam-c	5.45	1.33	0.24	1.51
sme-bantam-c*	2.73	3.09	1.13	1.24
sme-let-7a	2.42	5.82	2.4	5.12
sme-let-7a*	0.5	1.03	2.08	1.34
sme-let-7b	2.12	3.69	1.74	2.05
sme-let-7b*	1.82	3.09	1.7	1.02
sme-let-7c	1.37	1.48	1.07	1.35
sme-let-7c*	2.73	1.55	0.57	2.12
sme-let-7d	1.42	2.23	1.57	2.23
sme-let-7d*	2.73	1.55	0.57	2.7
sme-lin-4	2.03	2.12	1.04	1.25
sme-lin-4*	0.17	0.18	1.09	1
sme-miR-10	0.31	0.42	1.37	0.76
sme-miR-10*	0.09	0.15	1.57	0.81
sme-miR-10a	0.22	0.29	1.32	0.69
sme-miR-10a*	2.73	1.55	0.57	0.9
sme-miR-1175	0.17	0.15	0.86	0.44
sme-miR-1175*	0.19	0.39	1.99	0.66
sme-miR-12	0.07	0.07	0.88	0.72
sme-miR-12*	0.68	1.55	2.27	1.95
sme-miR-124a	0.49	0.41	0.84	1.09
sme-miR-124a*	1.36	0.77	0.57	0.84
sme-miR-124b	0.69	0.64	0.94	1.14
sme-miR-124b*	0.11	0.09	0.8	0.89
sme-miR-124c	0.53	0.51	0.98	1.01
sme-miR-124c*	0.55	0.77	1.42	1.24
sme-miR-124d	1.91	0.83	0.44	1.65
sme-miR-124d*	0.55	0.77	1.42	0.44
sme-miR-124e	0.45	0.77	1.7	0.99
sme-miR-124e*	1.82	1.55	0.85	0.64
sme-miR-125a	0.21	0.35	1.68	1.22
sme-miR-125a*	0.07	0.08	1.17	1.29
sme-miR-125b	0.86	0.95	1.11	1.27
sme-miR-125b*	2.73	0.52	0.19	1.21
sme-miR-13	4.88	4.57	0.94	5.46
sme-miR-13*	2.73	1.55	0.57	2.36
sme-miR-133	0.11	0.19	1.68	0.42
sme-miR-133*	0.15	0.18	1.19	0.72
sme-miR-133a	0.68	1.16	1.7	0.76
sme-miR-133a*	2.73	1.55	0.57	1.52
sme-miR-184	0.36	0.39	1.06	0.72
sme-miR-184*	0.11	0.42	3.71	0.69
sme-miR-190a	0.55	0.52	0.95	1.16
sme-miR-190a*	0.12	0.13	1.07	0.68
sme-miR-190b	0.39	0.77	1.99	1.06
sme-miR-190b*	0.12	0.13	1.16	0.75
sme-miR-1992	0.8	0.75	0.94	2.23
sme-miR-1992*	0.41	1.16	2.84	2.02
sme-miR-1993	0.22	0.34	1.58	0.66
sme-miR-1993*	0.23	0.52	2.27	0.65
sme-miR-1a	0.1	0.11	1.09	0.83
sme-miR-1a*	0.03	0.04	1.31	1.12
sme-miR-1b	0.28	0.29	1.03	0.81
sme-miR-1b*	0.07	0.07	0.96	0.84
sme-miR-1c	0.05	0.05	0.92	0.73
sme-miR-1c*	0.27	0.52	1.89	0.72
sme-miR-2147a	0.3	0.14	0.46	1.42
sme-miR-2147a*	2.73	1.55	0.57	1.15
sme-miR-2147b	0.71	1.16	1.63	1.06

miRNA	454, nb vs. un	454, nb vs ir	454, un vs. ir	solexa, un vs. ir
sme-miR-2147b*	2.73	1.55	0.57	3.54
sme-miR-2147c	0.41	0.34	0.84	1.23
sme-miR-2147c*	0.68	0.77	1.13	4.55
sme-miR-2148	0.12	0.52	4.35	1.31
sme-miR-2148*	0.68	1.55	2.27	1.77
sme-miR-2149	0.37	0.56	1.51	2.12
sme-miR-2149*	0.41	0.42	1.03	1.46
sme-miR-2150	0.18	0.19	1.06	1.5
sme-miR-2150*	0.45	1.55	3.4	0.63
sme-miR-2151	0.04	0.09	2.24	1.21
sme-miR-2151*	0.25	0.26	1.04	0.87
sme-miR-2152	65.99	8.51	0.13	0.21
sme-miR-2152*	2.73	1.55	0.57	0.1
sme-miR-2153	0.28	0.33	1.15	1.12
sme-miR-2153*	3.59	1.93	0.54	0.75
sme-miR-2154	0.05	0.09	1.67	0.77
sme-miR-2154*	0.91	1.55	1.7	0.66
sme-miR-2155	2.73	1.55	0.57	7.08
sme-miR-2155*	2.73	1.55	0.57	1.53
sme-miR-2156	0.23	0.33	1.42	0.77
sme-miR-2156*	0.68	0.39	0.57	0.7
sme-miR-2157	0.07	0.07	0.98	0.68
sme-miR-2157*	0.55	1.55	2.84	0.59
sme-miR-2158	0.02	0.02	0.92	0.71
sme-miR-2158*	0.34	0.77	2.27	0.49
sme-miR-2159	0.04	0.03	0.81	0.66
sme-miR-2159*	0.08	0.11	1.35	0.78
sme-miR-216	0.13	0.19	1.52	0.67
sme-miR-216*	0.04	0.06	1.45	1.1
sme-miR-2160	5.02	7.91	1.58	1.93
sme-miR-2160*	2.73	1.55	0.57	1.77
sme-miR-2161	0.61	0.73	1.21	0.7
sme-miR-2161*	2.73	1.55	0.57	1.77
sme-miR-2162	0.07	0.08	1.04	0.9
sme-miR-2162*	1.36	1.55	1.13	1.14
sme-miR-2163	0.34	0.34	1.01	1.02
sme-miR-2163*	1.36	1.55	1.13	1.33
sme-miR-2164	0.19	0.21	1.1	0.55
sme-miR-2164*	2.73	1.55	0.57	0.46
sme-miR-2165	0.91	1.55	1.7	0.93
sme-miR-2165*	1.36	0.39	0.28	0.72
sme-miR-2166	2.73	1.55	0.57	0.89
sme-miR-2166*	5.45	3.09	0.57	2.66
sme-miR-2167	0.3	0.31	1.02	0.79
sme-miR-2167*	2.73	1.55	0.57	0.89
sme-miR-2168	2.73	1.55	0.57	0.69
sme-miR-2168*	1.36	1.55	1.13	0.82
sme-miR-2169	2.73	1.55	0.57	1.1
sme-miR-2169*	2.73	1.55	0.57	0.68
sme-miR-2170	2.73	1.55	0.57	1.3
sme-miR-2170*	2.73	1.55	0.57	0.3
sme-miR-2171	1.36	0.39	0.28	1.36
sme-miR-2171*	2.73	1.55	0.57	0.44
sme-miR-2172	1.36	1.55	1.13	2.21
sme-miR-2172*	2.73	1.55	0.57	4.43
sme-miR-2173	2.73	3.09	1.13	1.15
sme-miR-2173*	1.36	1.55	1.13	1.77
sme-miR-2174	2.73	1.55	0.57	1.13
sme-miR-2174*	2.73	1.55	0.57	0.44
sme-miR-2175	2.73	1.55	0.57	0.89
sme-miR-2175*	2.73	1.55	0.57	1.77
sme-miR-2176	2.73	1.55	0.57	0.89
sme-miR-2176*	2.73	1.55	0.57	1.01
sme-miR-2177	2.73	1.55	0.57	1.42
sme-miR-2177*	1.36	1.55	1.13	1.77

miRNA	454, nb vs. un	454, nb vs ir	454, un vs. ir	solexa, un vs. ir
sme-miR-748*	2.73	1.55	0.57	0.53
sme-miR-749	0.93	0.84	0.9	0.65
sme-miR-749*	2.73	0.77	0.28	0.39
sme-miR-750	0.22	0.28	1.27	0.76
sme-miR-750*	0.39	0.52	1.32	0.89
sme-miR-751	0.21	0.77	3.69	0.96
sme-miR-751*	2.73	1.55	0.57	1.77
sme-miR-752	6.95	9.78	1.41	6.21
sme-miR-752*	1.64	0.66	0.41	1.44
sme-miR-753	0.68	1.55	2.27	1.63
sme-miR-753*	0.91	0.69	0.76	1.25
sme-miR-753b	0.3	0.77	2.55	1.72
sme-miR-753b*	1.2	1.55	1.28	1.21
sme-miR-754	0.11	0.19	1.7	0.41
sme-miR-754*	2.73	1.55	0.57	0.72
sme-miR-754b-1	0.14	0.24	1.7	0.78
sme-miR-754b-1*	2.73	1.55	0.57	2.21
sme-miR-754c	0.18	0.32	1.82	0.74
sme-miR-754c*	2.73	1.55	0.57	0.69
sme-miR-755	0.04	0.05	1.3	0.76
sme-miR-755*	0.03	0.04	1.23	0.77
sme-miR-756	2.02	2.26	1.12	1.57
sme-miR-756*	0.91	0.39	0.43	0.74
sme-miR-79	1.11	0.99	0.89	1.24
sme-miR-79*	0.55	1.55	2.84	1.49
sme-miR-7a	0.91	1.55	1.7	1.3
sme-miR-7a*	2.73	1.55	0.57	0.35
sme-miR-7b	0.8	1.19	1.49	1.35
sme-miR-7b*	2.73	1.55	0.57	1.59
sme-miR-7c	0.93	1.29	1.39	1.01
sme-miR-7c*	1.5	2.06	1.37	1.37
sme-miR-7d	0.88	0.7	0.8	1.97
sme-miR-7d*	1.36	0.77	0.57	0.89
sme-miR-8	1.37	1.57	1.15	0.89
sme-miR-8*	1.02	1.16	1.13	0.87
sme-miR-87a	0.27	0.24	0.89	1.08
sme-miR-87a*	0.23	0.18	0.76	0.71
sme-miR-87b	0.21	0.39	1.86	0.74
sme-miR-87b*	3.64	2.48	0.68	0.97
sme-miR-87c	0.1	0.08	0.81	0.93
sme-miR-87c*	0.55	0.44	0.81	0.79
sme-miR-87d	0.87	2.48	2.84	0.79
sme-miR-87d*	0.78	1.55	1.99	1
sme-miR-8b	0.36	0.5	1.38	0.82
sme-miR-8b*	2.73	1.55	0.57	1.18
sme-miR-92	0.34	1.03	3.03	0.81
sme-miR-92*	0.02	0.02	0.88	0.69
sme-miR-96a	0.14	0.13	0.95	0.92
sme-miR-96a*	2.73	1.55	0.57	0.76
sme-miR-96b	0.16	0.14	0.88	0.93
sme-miR-96b*	2.73	0.52	0.19	0.89
sme-miR-9a	0.17	0.22	1.3	0.71
sme-miR-9a*	2.73	1.03	0.38	0.84
sme-miR-9b	0.13	0.26	1.99	0.94
sme-miR-9b*	0.91	0.77	0.85	0.8
sme-putative-753.1	0.61	0.44	0.73	0.69
sme-putative-753.1*	0.78	0.28	0.36	1.07
sme-putative-753.2	0.91	0.42	0.46	1.1
sme-putative-753.2*	1.2	1.55	1.28	1.21
sme-putative-753.3	0.08	0.08	1.01	0.89
sme-putative-753.3*	2.73	1.55	0.57	0.73
sme-putative-753.4	0.08	0.08	1.01	0.89
sme-putative-753.4*	1.2	1.58	1.31	1.18
sme-putative-753.5	0.21	0.14	0.67	1.02
sme-putative-753.5*	1.2	1.58	1.31	1.22

Table S8. Sequences of the ³²P-radiolabeled oligodeoxynucleotides used as Northern blot probes for the validation of miRNA or piRNA candidates

SMECAND-02	AAC TTTT TGAATCACTACCTCT	>sme-miR-candidate-02 AGAGGUAGUGAUUCAAAAAGUU
SMECAND-05	AGTCAATTGATAATTTGCTCAT	>sme-miR-candidate-05 AUGAGCAAUUUAUCAAUUGACU
SMECAND-09	TCTGACCATATTGAGTGCAATC	>sme-miR-candidate-09 GAUUGCACUCAAUUAGGUCAGA
SMECAND-12	TGAATGTCTTAACTTTGCTCA	>sme-miR-candidate-12 GUGAGCAAAGUUUAAGACAUUCA
SMECAND-13	AGTAATACCCCAAGCAAC	>sme-miR-candidate-13 GUUGCUGGGGUUUUACU
SMECAND-15	ACCCACTTACCGCGTGCCTTA	>sme-miR-candidate-15 UAAGGCACGCGUAAGUGGGU
SMECAND-16	TGGCATTACAGCGTGCCTTA	>sme-miR-candidate-16 UAAGGCACGUGUGAAUGCCA
SMECAND-17	AGTATTCTTACCTGACAGTATTA	>sme-miR-candidate-17 UAAUACUGUCAGGUAAGAAUACU
SMECAND-18	CTCATGAATAACAGCATAATA	>sme-miR-candidate-18 UAUUAUGCUGUUUAUCAUGAG
SMECAND-19	ATGATTAATGTCTACCCGGTGA	>sme-miR-candidate-19 UCACCGGUAGACAUUAAUCAUG
SMECAND-20	GTCAATGGAACAAC TGTCTGA	>sme-miR-candidate-20 UCAGCAGUUGUCCAUGAC
SMECAND-21	ACACAATGCCAATTGTACAGCTGA	>sme-miR-candidate-21 UCAGCUGUACAAUUGGCAUUGUGU
SMECAND-23	TGAAAAGTTTAGGGGCCGTAAGA	>sme-miR-candidate-23 GGUAGGCAUAGUCUGUUGGUUAC >sme-piR-2618212
piR-2618212	CAT TCACTACTTCATTCTTTTCACATCCA	UUGGAUGUGAAAAGAAUGAAGUAGUGAAUGAG >sme-piR-1139655
piR-1139655	CTGTTGTTTATTAATTCCACATATTCAACTTA	UAAGUUGAAU AUGUGGAAUUAUAAACAACAGUU >sme-piR-2038493
piR-2038493	GCAATCGACCTCCAACGATAATCTTCGCA	UGCGAAGAUUAUCGUUGGAGGUCGAUUGCCC >sme-piR-1816361
piR-1816361	TGGGTATTTGTGTTTCATAGCACTTGCTTCA	UGAAGCAAGUGCUAUGAACACAAAUACCCA